Sudan University of Science and Technology
College of Graduate Studies
College of Engineering and Technology of Industries

Effect of Loop Lengths on Negative Poisson's Ratio of Weft knitted Fabric Reinforced Epoxy Composite

تأثير أطوال العراوي على نسبة بويزون السالبة للمواد المركبة المصنعة من قماش تريكو اللحمة والايبوكسي

Thesis submitted in fulfillment of the requirements for the Degree of M.Sc. in fiber and polymer engineering

Name of the Scholar:

Nada Osman Mohamed farh

Supervisor:

Dr. Ramadan Mohammed Ahmed.

May 2019

ايات من الذكر الحكيم

{ مَثَلُ الَّذينَ اتَّخَذُوا منْ دُون اللَّه أَوْلياءَ كَمَثَل الْعَنْكَبُوت اتَّخَذَتْ بَيْتًا وَإنَّ أَوْهَنَ الْبُيُوت لَبَيْتُ الْعَنْكَبُوت لَوْ كانُوا يَعْلَمُونَ (41) إنَّ اللَّهَ يَعْلَمُ ما يَدْعُونَ منْ دُونه منْ شيء وَهُوَ الْعَزيزُ الْحَكيمُ (42) وَتلْكَ الْأَمْثالُ نَضْربُها للنَّاس وَما يَعْقلُها إلاَّ الْعالمُونَ (43) خَلَقَ اللَّهُ السَّماوات وَالْأَرْضَ بالْحَقّ إنَّ في ذلكَ لَآيَةً للْمُؤْمنينَ (44)} **سورة العنكبوت: الآيات [41-44]**.

ACKNOWLEDGEMENTS

First of all, I would like to express my deepest appreciation to my supervisor, **Dr. RAMADAN MOHAMMED AHMED**, for academic guidance, efficient instructive advice and valuable help during my study.

I would like to thank my Teachers, A. Abdel Azeez, A. Adel ahmed and A. Adel saty and all Teachers in textile engineering department for their suggestions and help.

I should also thank Donghua University for wonderful collaboration to help in manufacture specimens.

Thanks from the depths for Dr. Magdi Al Amin, and Engineering Ammar Salah.

I also would like to thank my friends and colleagues for their help and kindness during my study, especially thanks to: Omniyat, Marwa, Wesal, Anfal, Salma, Somia, Omsalma, Muaz al amen and others.

I would like to express my special thanks to my parents, my sisters and brothers, for their unlimited support, love and sacrifice.

ABSTRACT

Conventional fabrics usually exhibit a positive poisons ratio (PR), i.e. they laterally shrink when stretched and laterally expand when compressed. On the contrary, auxetic fabrics exhibit a negative PR, i.e., they laterally expand when stretched or laterally shrink when compressed .The auxetic behavior equips fabrics with a lot of enhance properties.

The Negative Poisson Ratio (auxetic) based on Weft knitted fabric can have huge potential for applications, especially in personal protection materials like bullet proof vest, and many industries application such as air space, automobile, and so on.

This study presents use of NPR weft knitted fabric in composite materials using polypropylene yarns through the weft knitted technique. The polypropylene filament yarn knitted on flat knitting machine (Passap Deumatic 80), as a rib structure (fisherman's rib) with three different loop lengths (LL3, LL4, and LL5).

Investigation of the effect of different loop lengths on the negative Poisson ratio (NPR) in the wale and course direction.

The result showed that all knitted fabrics have NPR effect, for the both direction.

The composite material manufactured employed NPR weft knitted fabric using Risen Transfer Molding (RTM) process.

Tensile strength and low velocity impact tests are performed to determine the load-extension and the amount of energy absorbed in the wale and course direction.

The result showed that the LL5 have the highest extension and displacement, and LL3 have the highest load bearing.

The failure modes of impact test characterized as combinations of matrix cracking, surface buckling, delamination, and fiber fracture. As the impact energy is increased, the area of composite deformation increases.

المستخلص

عادة ما تُظهر الأقمشة التقليدية نسبة بواسون الموجبة (PR) ، أي أنها تتقلص بشكل جانبي عندما تمدد وتتوسع أفقياً عند ضغطها. على العكس من ذلك ، تُظهر الأقمشة (الأوكسيتك) نسبة بواسون السالبة (NPR)، أي أنها تتوسع أفقياً عند التمدد أو الانكماش الجانبي عند الضغط.

نسبة بواسون السالبة (auxetic) التي تعتمد على قماش تريكو اللحمة لديها إمكانات هائلة للتطبيقات, تحديدا في مواد الحماية الشخصية مثل سترة واقية من الرصاص ، والعديد من التطبيقات الصناعية مثل الطائرات والسيارات .

تعرض هذه الدراسة إستخدام قماش تريكو اللحمة (auxetic) في المواد المركبة بإستخدام خيط البولي بروبيلين, تم نسج خيوط البولي بروبلين على ماكينة التريكو المسطحة (الباساب), بتركيب مضلع (fisherman's rib) بثلاثة اطوال عراوي مختلفه (LL3, LL4, LL5).وتم إختبار تأثير أطوال العراوي المختلفه على نسبة بواسون السالبة (NPR) في اتجاة الطول والعرض. وأظهرت النتائج أن جميع أقمشة التريكو لها تأثير على NPR في الاتجاهين.

تم تصنيع مادة مركبة بإستخدام قماش تريكو اللحمة (NPR) بطريقة RTM. وإجراء إختبارات قوة الشد والاصطدام بسرعة منخفضة , لتحديد امتداد الحمل وكمية الطاقة التي يتم امتصاصها في اتجاة الطول والعرض. وأظهرت النتائج أن LL5 أعلى استطالة وازاحة، و LL3 الأكثر تحملا للحمل.

تم وصف أوضاع الفشل في اختبار التصادم على أنها مزيج من تكسير الماتركس ، إنبعاج السطح, فصل طبقات, وكسر الألياف. ومع زيادة تأثير الطاقة ، زادت مساحة التشوه للمادة المركبة.

TABLE OF CONTENT

CHAPTER ONE- INTRODUCTION

CHAPTER TWO -LITERATURE REVIEW

CHAPTER THREE-MATREIAL AND METHOD

CHAPTER FOUR-RESULT AND DISCUSSION

LIST OF TABLES

LIST OF FIGURES

CHAPTER ONE

INTRODUCTION

1.1 Background:

Definition of Poisson's Ratio (PR), Poisson's ratio is the ratio of transverse contraction strain to longitudinal extension strain in the direction of stretching force. Tensile deformation is considered positive and compressive deformation is considered negative (Hursa et al., 2009).

Conventional fabrics usually exhibit a positive poisons ratio (P R), (they laterally shrink when stretched and laterally expand when compressed. Auxetic fabrics exhibit a negative (P R),(they laterally expand when stretched or laterally shrink when compressed (Wang and Hu, 2015), as shown in Fig (1.1).

1.1.1 Auxetic textiles:

Auxetic textiles are materials which possess negative Poisson's ratio, this implies that in contrast to conventional textile materials if they are stretched in longitudinal direction, a marginal expansion will results in transversal direction. Auxetic textile materials have become a point of focus for many researchers in recent past years. Their achievements in the area of auxetic textile materials including fibers, yarns, fabrics and textile reinforcements for composite applications (Hu, 2016, Steffens et al., 2016).

The NPR effect of a material normally comes from its special structural arrangement. To date, a variety of special geometrical structures have been discovered for making NPR materials from the macroscopic level down to the molecular level. Among the most important classes of these NPR structures, it is possible to cite re-entrant structures (Grima et al., 2005), chiral structures (Spadoni et al., 2005), rotating units(Grima et al., 2007), angle-ply

laminates(Milton, 1992), hard molecules(Tretiakov and Wojciechowski, 2007), micro porous polymers (Alderson et al., 2007), and free rod liquid crystalline polymers (He et al., 2005).

Negative Poisson's ratio (NPR) materials are different from most conventional materials. They exhibit the very unusual property of becoming wider when stretched and narrower when compressed(Evans et al., 1991),This counterintuitive behavior gives NPR materials various beneficial effects, such as enhanced shear stiffness, increased plane strain fracture toughness, increased indentation resistance, and improved energy absorption properties (Evans and Alderson, 2000b),(Yang et al., 2004).

The Advantage of Auxetic materials:

Auxetic materials are of particular interest due to:

- Their counterintuitive behavior under strain.
- Improved enhanced strength.
- Better acoustic behavior
- Improved fracture toughness
- Superior energy absorption.
- Damping improvement.
- Indentation resistance (Carneiro et al., 2013a).

Types of auxetic materials

The main types of auxetic materials are:

- Auxetic bio-materials.
- Auxetic foams.
- Auxetic honeycombs.
- Auxetic polymers.
- Auxetic structures.

- Auxetic composites (Evans and Alderson, 2000b).

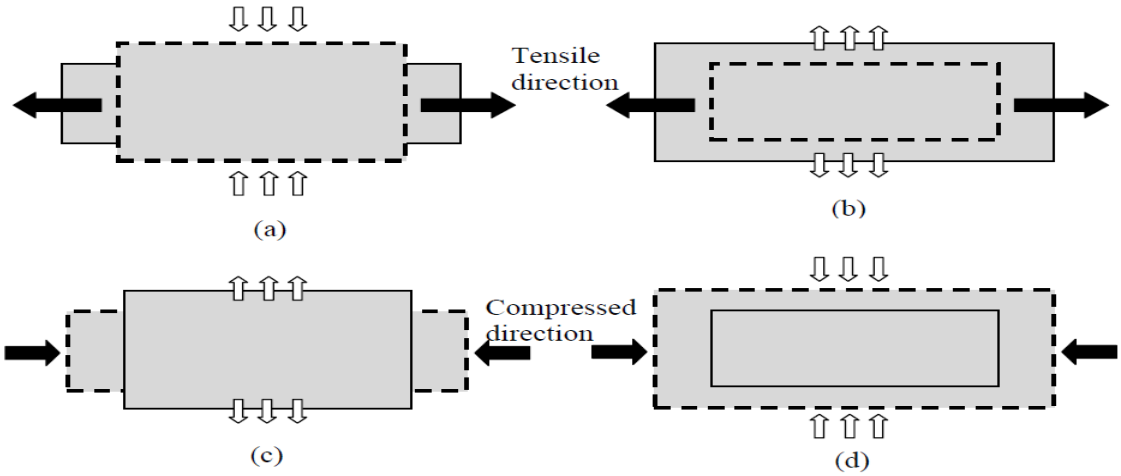

Fig (1.1): Stretch/compression behaviors of (a)/(c) conventional, and (b)/(d) auxetic fabrics.

1.1.2 Auxetic composites:

Auxetic composites have better performance than conventional composites and have some special applications; Auxetic composites are a special kind of composites that have a negative PR. They laterally expand when stretched or laterally shrink when compressed in the longitudinal direction. They also can be made from auxetic materials, for example by using auxetic inclusions with different geometry, proportions and properties to make the final composites possess auxetic properties (Rana and Fangueiro, 2016).

Advantages and disadvantages:

Auxetic composites have many advantages, such as high specific stiffness, high specific strength, light weight, higher shear, enhanced indentation resistance, better crack resistance and higher damping resistance. Auxetic composites have a high strength-to-weight ratio. We know that the weight saving is extremely important for aircraft and that both energy consumption and pollution can be reduced by

lowering the aircraft weight. Performance and safety can also be improved. Another advantage of auxetic composites is that the auxetic property and strength can be customized by changing the component's proportions. With different components and manufacturing methods, specific auxetic composites can be made for desired usages.

The disadvantage of auxetic composites is that they are difficult to manufacture on a large scale (Wang et al., 2016).

1.2 Composite material:

Composites, which consist of two or more separate materials combined in a structural unit, are typically made from various combinations of the other materials (Gibson, 2011).

Typical engineered composite materials include:

- Composite building materials, such as cements, concrete
- Reinforced plastics, such as fiber-reinforced polymer
- Metal composites
- Ceramic composites (composite ceramic and metal matrices)

Composite materials are generally used for buildings, bridges, and structures such as boat hulls, swimming pool panels, race car bodies shower stalls, bathtubs, storage tanks, imitation granite and cultured marble sinks and countertops. The most advanced examples perform routinely on spacecraft and aircraft in demanding environments .

1.2.1 Classification of composite material:

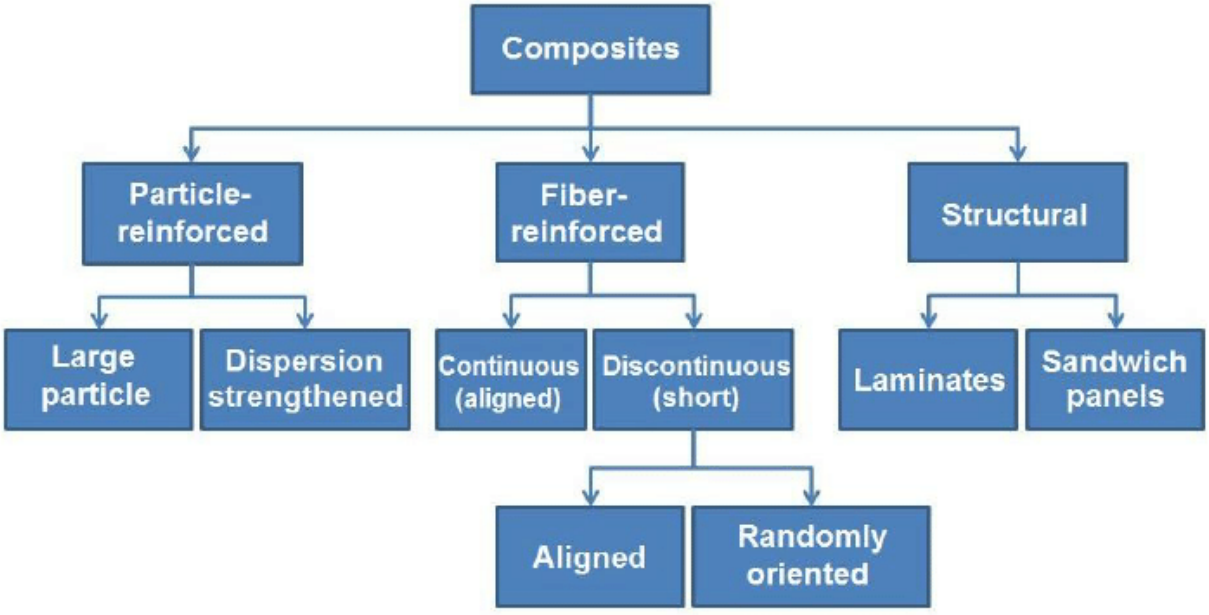

Fig (1.2): Classification of composite material (Daniel et al., 1994).

1.2.2 Structure of Composites:

Structure of a composite material determines its properties to a significant extent. Structure factors affecting properties of composites are as follows:

- Bonding strength on the interface between the dispersed phase and matrix.
- Shape of the dispersed phase inclusions (particles, flakes, fibers, laminates).
- Orientation of the dispersed phase inclusions (random or preferred).

Good adhesion (bonding) between matrix phase and displaced phase provides transfer of load applied to the material to the displaced phase via the interface. Good adhesion is required for achieving high level of mechanical properties of composites. Very small particles less than0.25 micrometer finely distributed in the matrix impede movement of dislocations and deformation of the material. They

have strengthening effect. Large dispersed phase particles have low share load applied to the material resulting in an increase of stiffness and decrease of ductility.

1.2.3 Laminates:

A composite laminate is an assembly of layers of fibrous composite materials which can be joined to provide required engineering properties, including in-plane stiffness, bending stiffness, strength, and coefficient of thermal expansion.

The individual layers consist of high-modulus, high-strength fibers in a polymeric, metallic,or ceramic matrix material.

Layers of different materials may be used, resulting in a hybrid laminate. The individual layers generally are orthotropic (that is, with principal properties in orthogonal directions) or transversely isotropic (with isotropic properties in the transverse plane) with the laminate then exhibiting anisotropic (with variable direction of principal properties) (Talreja and Singh, 2012).

1.3 Knitted composites:

They are composite that knitted fabric acts as a reinforcement embedded in a matrix. They possess attractive properties for niche applications, requiring high energy absorption or good impact resistance, or in cases where the component is complex in shape and demands exceptional formability.

The lack of a comprehensive understanding of the way knitted composites behave still acts as an impediment to the wider acceptance of the material and, hence, expanded application (Gulhane et al., 2014).

1.3.1 Classification of knitting technology:

Knitting technology is classified into two main groups according to yarn presentation and yarn processing:

1- Weft knitting technology.
2- Warp knitting technology.

In weft knitting technology, one yarn end is horizontally fed into all needles in the needle bed (Raz, 1991).

Products obtained from weft knitting technology are widely used in the apparel industry for pull-over's , t-shirts, sweatshirts, etc (Horrocks and Anand, 2000).

Weft knitting machines have relatively low investment cost, small floor space requirements, low stock holding requirements and quicker pattern change capabilities than warp knitting machines.

Flat knitting is a widely used fabric manufacturing technology. Compared with warp knitting and circular knitting, flat knitting is characterized by its higher process flexibility and greater fabric structure variety. Auxetic fabrics can be realized based on knitted structures and that flat knitting technology can provide a simple, but highly effective way of fabricating auxetic fabrics from conventional yarns (Hu et al., 2011). In warp knitting technology, one yarn end is longitudinally fed into one needle in the needle bed. Products obtained from warp knitting technology are widely used for household and technical textiles such as geotextiles, curtains, toweling ,etc(Raz, 1987).

1.4 Applications:

Auxetic materials can be used in various areas, including medicine, architecture, civil engineering, sport clothing, high-performance equipment, protection against explosives, insulation, filters, among others (Evans and Alderson, 2000a, Alderson and Alderson, 2005, Simkins et al., 2005, Liu, 2006, Prawoto, 2012, Wright et al., 2012, Subramani et al., 2014).

The NPR composites developed within this work present great potential for applications in industrial areas, including personal protection products, such as bulletproof vests, helmets, elbow protectors, and helicopters, transportable shelters,

shin pads and knee pads, and in all other areas where energy absorption is a key factor to be considered (Steffens et al., 2017, Jacobs and Van Dingenen, 2001, Yang et al., 2004).

1.5 Objective:

The aims of this study are:

1- To fabricate a new kind of auxetic fabric with good and stable auxetic effect using weft knitting technology.
2- To learn the principle of the auxetic fabric suitable for weft knitted fabric based on a basic understanding of relationship between the structure properties and auxetic effect of different loop length.
3- To develop special knitting and post-processing method for producing NPR weft knitted fabric composite based on the designed structure.
4- To conduct appropriate structure to predict the deformation behavior of the NPR weft knitted fabric composite.

1.6 Thesis outline:

Chapter 1 gives introduction, application, and objective of this thesis.

Chapter 2 reviews the relevant literatures to get a general understanding of the background. The limitations and gaps of the previous works are found out and the objective of the research work is identified.

Chapter 3 introduces the manufacturing of NPR weft knitted fabrics with three different loop lengths and the NPR weft knitted composite laminate. Present an experiment study of the effect for different loop lengths on the NPR.

Chapter 4 presents an experiment study of the NPR value for wale and course direction from this fabric, the effect of loop length for NPR, and tensile, impact properties of the NPR weft knitted fabric composite.

Chapter 5 presents the conclusion, and recommendations for future work.

CHAPTER TWO

LITERATURE REVIEW

2.1 Historical Background:

This chapter reviews the area of auxetic textile materials including fibers, yarns, fabrics and textile reinforcements for composite applications. It is aimed that this review will be helpful for future advancement in the area of auxetic textile materials (Hu, 2016).

Auxetic materials are endowed with a behavior that contradicts common sense, when subjected to an axial tensile load they increase their transverse dimension. In case of a compression load, they reduce their transverse dimension .These materials have a negative Poisson's ratio (NPR) in such direction (Carneiro et al., 2013b).

2.2 Classification of Auxetic material:

2.2.1 Auxetic fibers and polymers

Uzun and Patel were manufactured auxetic and conventional PP fibers from Coathylene PB0580 powder, produced by DuPont Polymer Powders (Sarl, Switzerland) and supplied by Univar (Bradford, UK). Auxetic and conventional PP fibers have been produced by the melt spinning technique using previously established processing parameters, and produced Plain knitted fabric structure. Results obtained on the abrasion resistance of both the auxetic and conventional PP fiber based knitted fabrics have been compared.They showed that auxetic PP knitted fabric has better abrasive wear resistance (15-35%) than conventional PP knitted fabric (produced at 200°C and over) as shown in the SEM image in Fig(2.1) (Uzun and Patel, 2010).

Uzun, M., had produced of composites, from auxetic and conventional polypropylene (PP) fibers were produced by the melt spinning technique. The fibers which were tested and analyzed in terms of Poisson's ratio, linear density, elongation at break and tenacity as shown in Table (2.1).The auxetic and conventional PP stable fiber reinforced composites were fabricated by the hand layup method. Several mechanical properties of the composites were examined, including tensile strength, Young's modulus, elongation at break, energy absorption, impact velocity and damage size. It was found that the auxetic fiber reinforced composites (7.5% and 10%) had the highest tensile strength and the auxetic fiber reinforced composite (5%) had the highest Young's modulus. The highest energy absorption was observed for the composite made with 10% auxetic fiber loading (Uzun, 2012).

Table (2.1): Auxetic and conventional PP fibers properties.

Parameter	**Auxetic PP (159 °C)**	**Conventional PP (170 - 230 °C)**
Diameter, tex	40	40
Elongation at break,%	2.17	4.66
Tenacity, cN/tex	3.19	2.32
Poisson’s ratio values	-0.70 to -0.40	-0.12 to + 0.35

Pickles, A., K. Alderson, and K. Evans With the use of a three-stage thermal processing route, similar to that used previously for the production of ultra high molecular weight polyethylene possessing a negative Poisson's ratio (i.e. displaying auxetic behavior), an auxetic form of polyethylene has been fabricated. The polypropylene is processed by the compaction, sintering, and

extrusion of a powder. The importance of powder morphology on the ability of polypropylene to achieve auxetic behavior has been examined, revealing that particle shape, size, and surface roughness are critical variables for successful processing. Negative Poisson's ratios of up to −0.22 at 1.6% strain have been obtained (Pickles et al., 1996).

Bertoldi , K., et al. produced particular form of ultra-high molecular weight polyethylene (UHMWPE) capable of exhibiting large negative Poisson's ratio (ν) because of its complex microstructure .It was found that the presence of a negative ν resulted in enhancements of the hardness by up to a factor of 2 over conventional UHMWPE (Bertoldi et al., 2010).

Alderson.A et al. produced polymeric monofilaments displaying auxetic behavior. The structure and deformation mechanisms at the micro scale, rather than at the molecular level (as compared to conventional filaments extruded from a fully molten polymer) are responsible for enhanced mechanical properties, including the auxetic effect. In another study,they produced auxetic poly propylene fibers by using thermal processing technique (Alderson and Evans, 2002). A large value of Poisson's ratio (v = -0.6) was obtained when measured by using video extensometer (Alderson and Alderson, 2005).

Wright, J.R., et al developed low-stiffness auxetic yarns and fabrics which offer a range of applications such as medical devices, particularly bandages, compression hosiery and support garments and fashion apparel. A yarn Poisson's ratio as low as −1.5 is demonstrated, and fabrics with in-plane and out-of-plane negative Poisson's ratios are illustrated. Stiffness is shown to be highly dependent upon yarn geometry (Wright et al., 2012).

Underhill, R. discussed some of the unique physical properties of auxetic materials and various approaches to achieving them. The key to using auxetic materials in future applications is their successful synthesis and development.

Despite an abundance of papers on the theory of auxetic materials, at present only microporous foams and yarns have shown negative Poisson's ratios experimentally. A successful auxetic material will be one which can be produced on a commercial-scale, with the desired properties (Underhill, 2014).

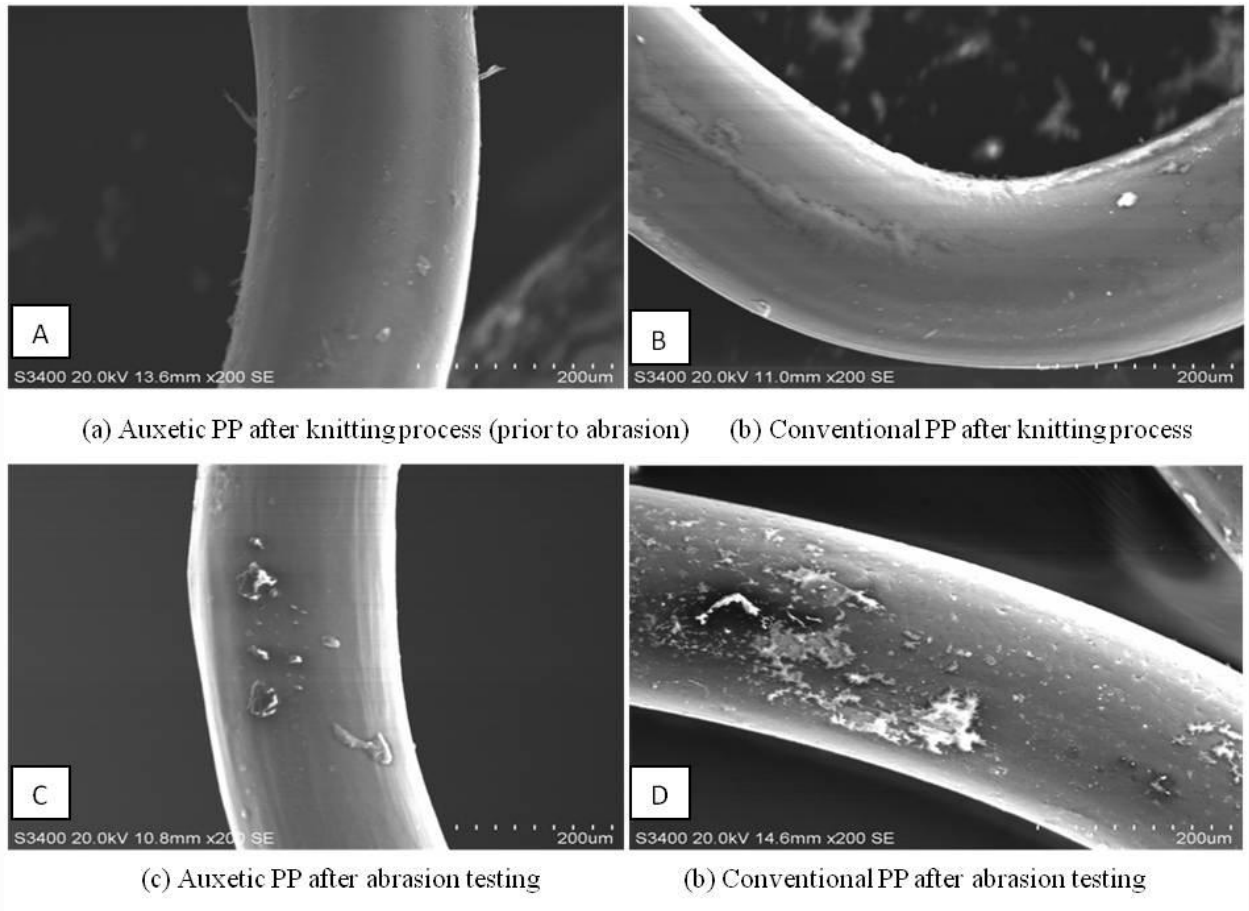

Fig (2.1): SEM images of auxetic and conventional PP fibers surface (200 c^{o})

2.2.2 Auxitec Fabric:

Ugbolue et al produced knit structures made of conventional yarns by using chain and filling yarn inlays. They combined the principles of geometry, fabric structural characteristics and conventional elastic yarn to engineer hexagonal knit structures with negative Poisson's ratio (Ugbolue et al., 2014).

A low in stiffness and thick filament was used for open looped wales while, a high stiffness filament is inlaid around the under lap loops Fig (2.2a). Upon stretching the high stiffness filament get straight and becomes fully aligned causing the open loops of lower stiffness filament to wrap around the straightened high stiffness filament as shown in Fig (2.2b) exhibiting the auxetic behavior. Auxetic properties can be observed in the resultant structure by mingling two or more of these wale in some suitable manner as shown in Fig (2.2c). The resultant functional auxetic knit structure is shown in Fig (2.2d).

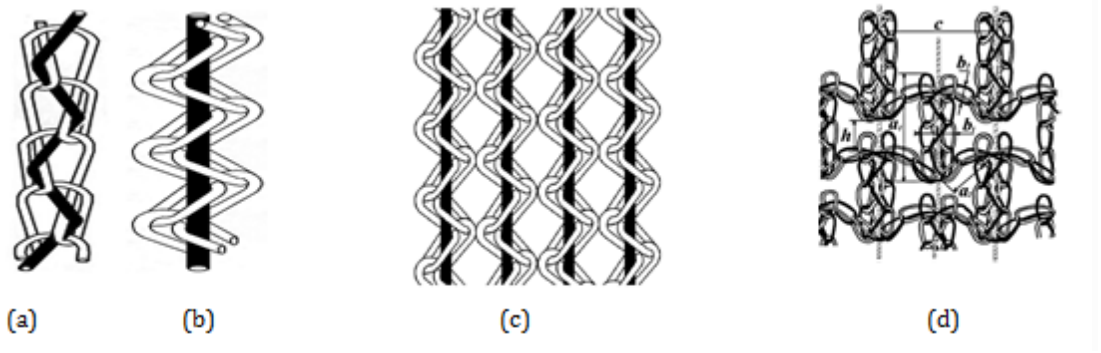

Fig (2.2): Warp knit structures from wale of chain and in lays yarn (Ugbolue et al., 2014).

Flat knitting technology was exploited to fabricate auxetic fabrics which laterally expand when stretched. Hu, H., Z. Wang, and S. Liu, investigated three kinds of geometrical structures, i.e. foldable structure (Darja et al., 2014), rotating rectangle (Grima, 2010)and re-entrant hexagon (Assidi and Ganghoffer, 2012). The results reveal that except the folded fabric formed with the face loops and reverse loops in a rectangular arrangement, of which the auxetic effect firstly increases and then decreases with the axial strain shown in Fig (2.3) (Hu et al., 2011).

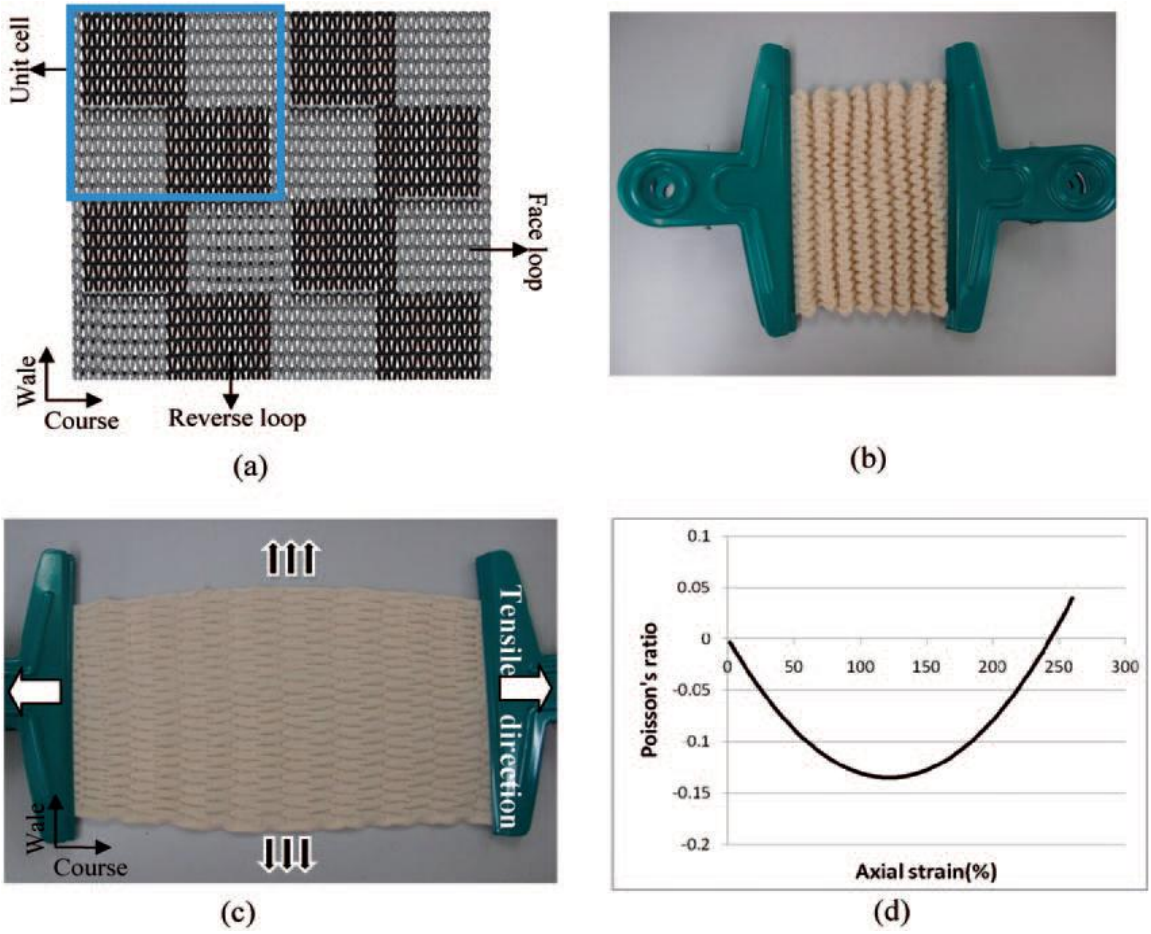

Fig (2.3): Auxetic fabric formed with the arrangement of face and reverse loops in rectangular forms. a) Knitting pattern, b) fabric at the free state, c) fabric at the stretched state, d) Poisson's ratio vs. strain (Hu et al., 2011).

Foldable structures:

A folded structure can be unfolded when stretched in one direction this principle was used to create a range of weft knitted auxetic fabrics. Recently, a range of auxetic knitted fabric has been produced by using weft flat knitting technology (Liu et al., 2010, Liu and Hu, 2010).The development was based on a geometrical analysis of a new three dimensional structure that can yield negative Poisson's ratio (auxetic effect). They employed a three-dimensional structure formed with

parallelogram planes of the same shape and size connected together side to side in a zigzag format as shown in Fig (2.4). When stretched either in horizontal or vertical direction, each parallelogram changes its inclined position related to the surface plane of the structure, which results in an opening of the whole structure by increasing its dimensions in both the horizontal and vertical directions. Therefore, the auxetic effect is observed while the shape and size of the parallelogram planes remain unchanged. This auxetic effect comes from the opening of the folded structures in both course and wale directions, exactly like the structure shown in Fig (2.4).

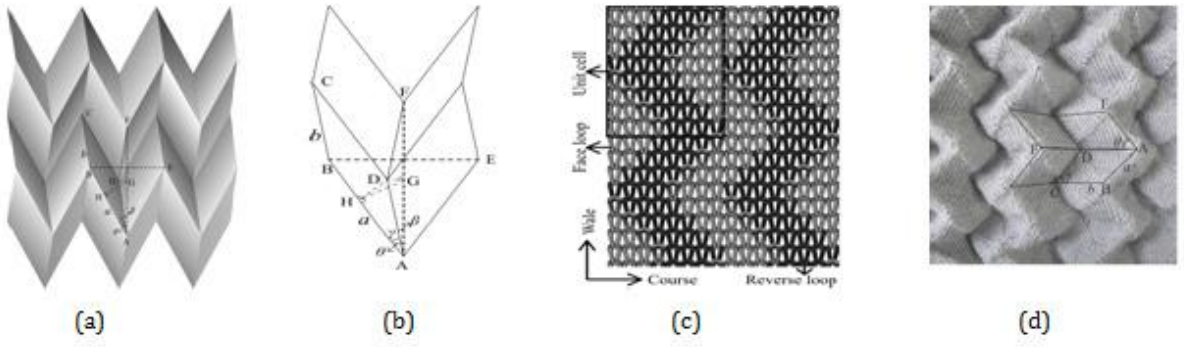

Fig (2.4) : (a) Three-dimensional structure; (b) unit cell (c) Knit pattern (d) Stretched state of the knitted fabric (Liu et al., 2010).

Rotating Rectangles:

Several studies have revealed that an auxetic effect can successfully be induced by using rotating units such as rectangles(N. Grima et al., 2005), triangles(Grima and Evans, 2006), rhombi (Attard and Grima, 2008) and parallelograms(Attard et al., 2009). One such example based on rigid rectangles connected together at their vertices by hinges is demonstrated in Fig (2.5). Based on the same geometrical arrangement, an auxetic fabric was produced by Hong H et al(Hu et al., 2011).

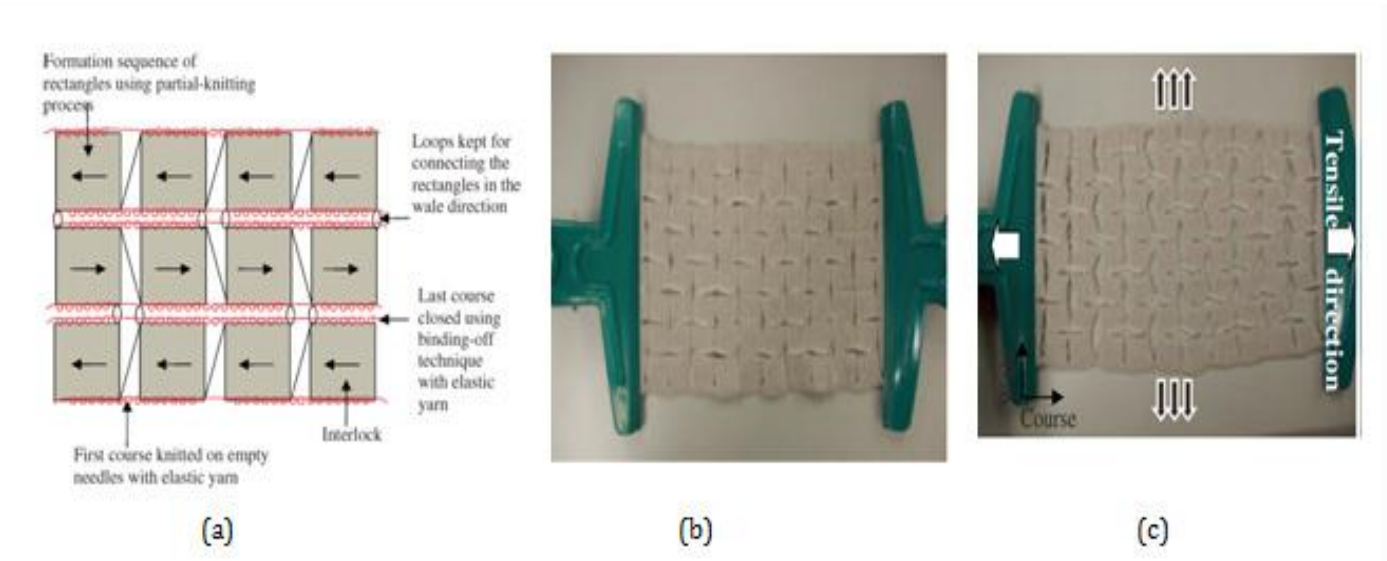

Fig (2.5): Auxetic fabric formed with rotating rectangles. (a) Schematic presentation of knitting process (b) fabric at the free state(c) fabric at the stretched state.

Re-entrant hexagonal structure:

A number of studies have revealed the potential of reentrant hexagonal geometries in order to induce the auxetic behavior. One such geometry is shown in Fig (2.6) and Fig (2.7).

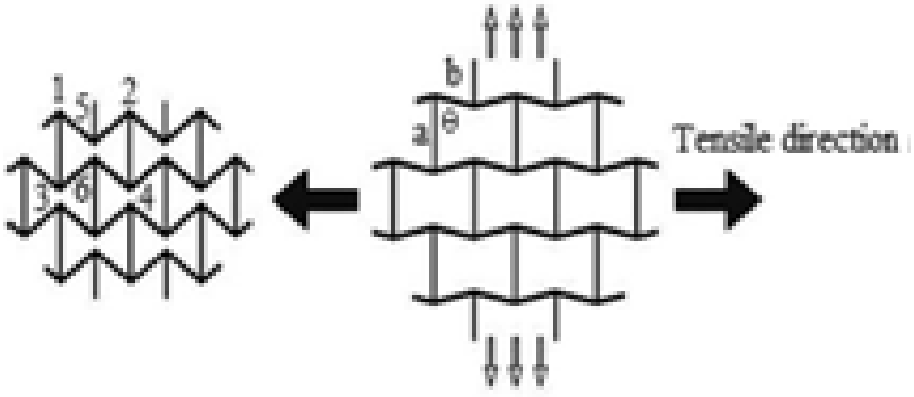

Fig (2.6): Reentrant hexagonal structure.

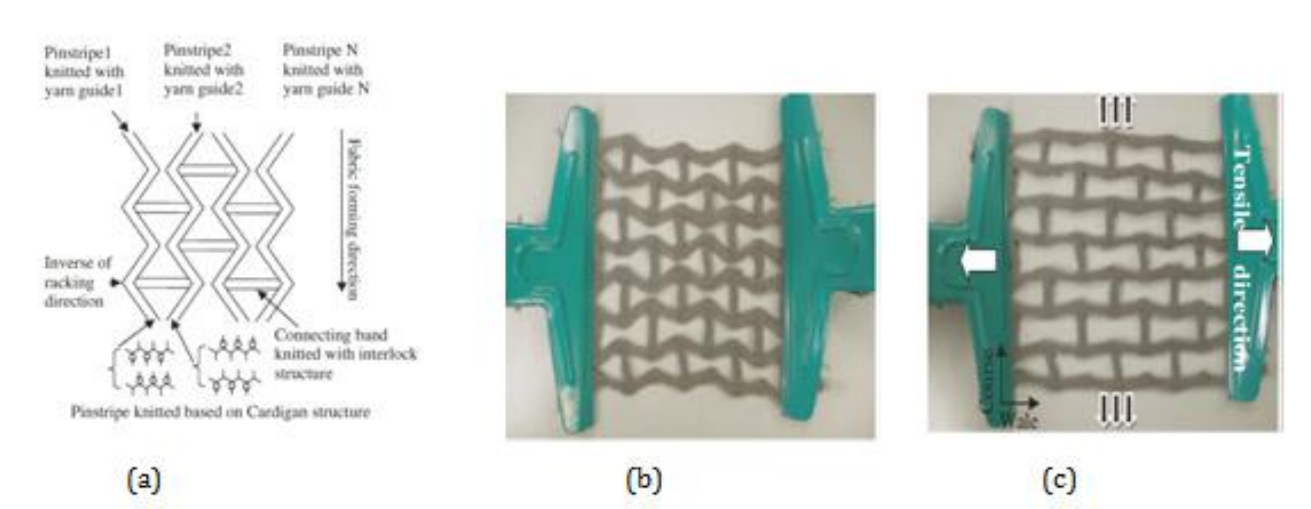

Fig (2.7): Auxetic fabric formed with real reentrant hexagonal structure. (a) Schematic presentation of knitting process(b) fabric at the free state(c) fabric at the stretched state (Hu et al., 2011).

In Fig (2.8) auxetic fabric was a pseudo-re-entrant hexagonal structure produced using sectional relief ridges in the combination with elastic yarn.

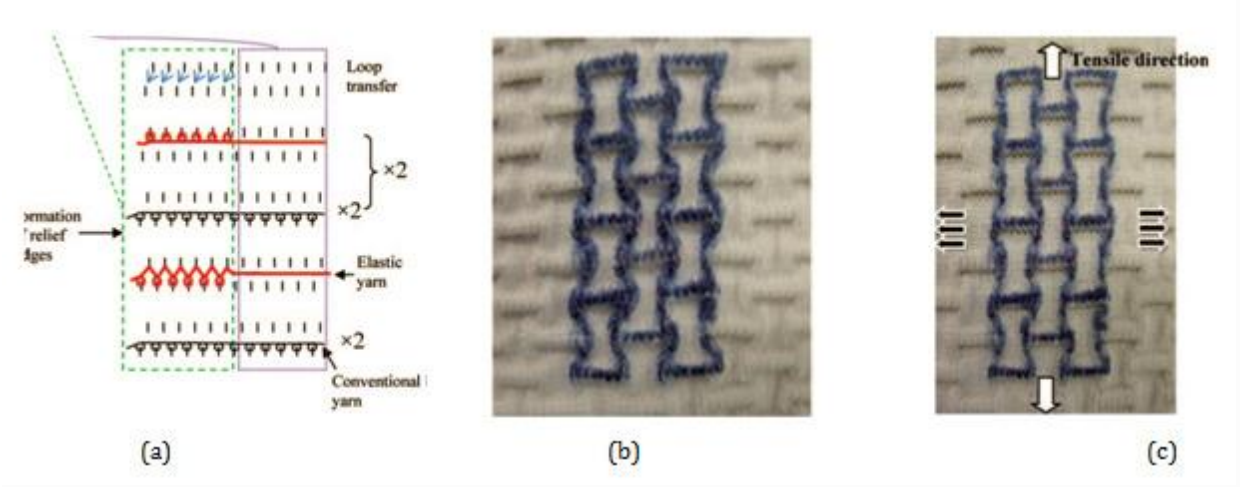

Fig (2.8): Auxetic fabric formed with pseudo-reentrant hexagonal structure. (a) Schematic presentation of knitting process (b) fabric at the free state (c) fabric at the stretched state (Hu et al., 2011).

2.2.3 Auxetic Composites:

Developments in auxetic materials production have made it possible to produce auxetic fiber reinforced composites. Miller W et al reported that an auxetic composite can be produced by using a woven auxetic fabric made of auxetic yarns. The reinforcement for an auxetic composite can be made using a double helix yarn (DHY). The auxetic behavior of DHY yarns can be reserved into a woven fabric if the pitch levels between adjacent yarns in the fabric and material properties are optimized illustrated in Fig (2.9) (Miller et al., 2009).

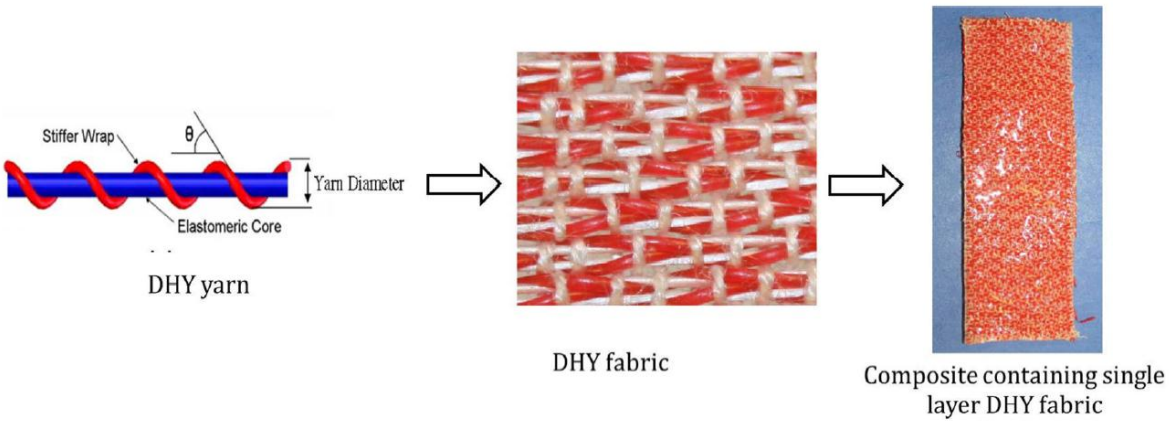

Fig (2.9) Production of auxetic composites from DHY

Steffens et al was fabricated Composites using weft knitted fabrics made from high performance yarns such as Para aramid and ultra-high-molecular-weight polyethylene (Spectra). These auxetic fabrics were impregnated with epoxy and unsaturated polyester resins based on iso-phthalic acid. The produced composites with Para - aramid fibers exhibited excellent impact strength and energy absorption characteristics and considered to be highly suitable for advanced technical applications as shown in Fig (2.10) (Steffens et al., 2016).

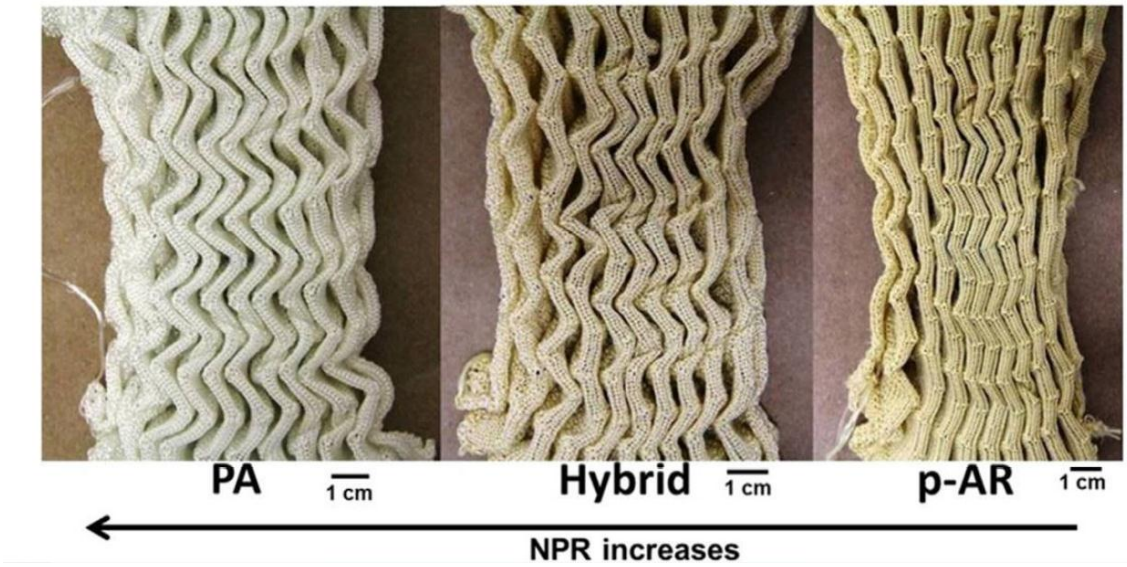

(a)

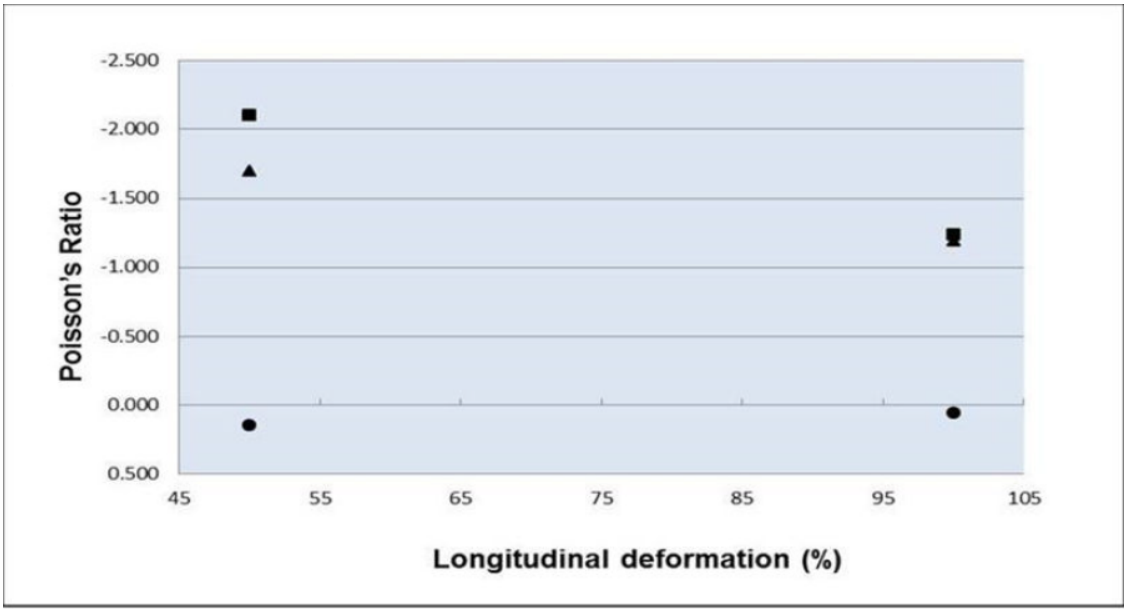

(b)

Fig (2.10): (a) auxetic fabrics produced using polyamide (PA), para aramid (p-AR) and hybrid yarns and (b) Poisson's ratio of developed fabrics.

2.2.3.1 Two -D Auxetic textile structure for composite reinforcement:

Cabras, L. and M. Brun, proposed a class of lattice structures with macroscopic Poisson's ratio arbitrarily close to the stability limit −1; the uniaxial test and, a theoretical analysis of the effective properties were performed, and the expression of the macroscopic constitutive properties is given in full analytical form as a function of the constitutive properties of the elements of the lattice and on the geometry of the microstructure (Cabras and Brun, 2014).

2.2.3.2 Three -D Auxetic textile structure for composite reinforcement:

Ge Z et al had produced A novel 3-D auxetic (negative Poisson's ratio) textile structure for composite reinforcement which shrinks when compressed.

They combined the non-woven and knitting technology with conventional yarns and produced some novel 3D auxetic fabric reinforcements that could be utilized as preform to produce auxetic composites. The novel 3D auxetic fabric structure as shown in Fig (2.11) is composed of three yarn systems, i.e. weft yarns, warp yarns and stitch yarns (Ge and Hu, 2013).

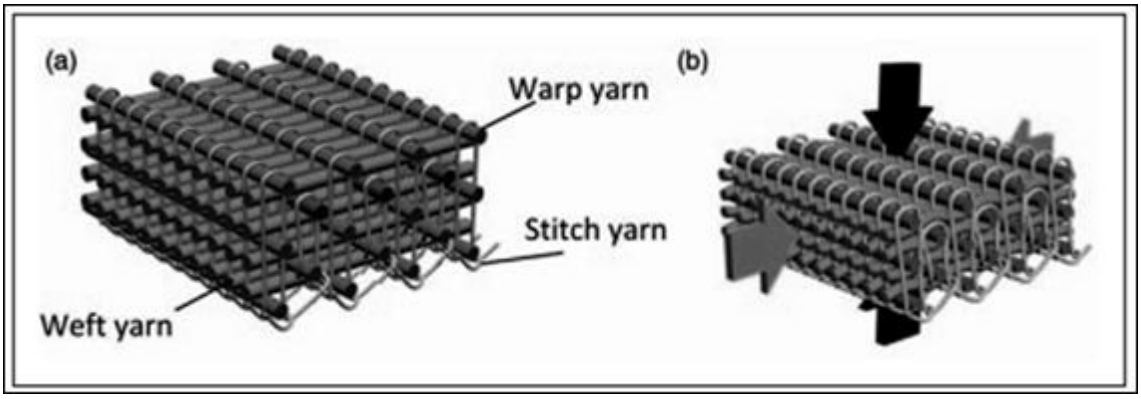

Fig (2.11): Three dimensional auxetic textile structure (a) Initially (b) Under compression (Ge and Hu, 2013).

Steffens, F., et al developed polymeric composite materials reinforced with auxetic knitted fabrics and evaluated the degree of transference of the auxetic behavior from the fibrous reinforcement to the composite produced. The results showed that the NPR values remained in the composites. Regardless of the type of resin used, either epoxy or polyester, the highest values were obtained for samples produced with p-AR auxetic knitted fabrics(Figs 2.12 , 2.13 and 2.14) (Steffens et al., 2017).

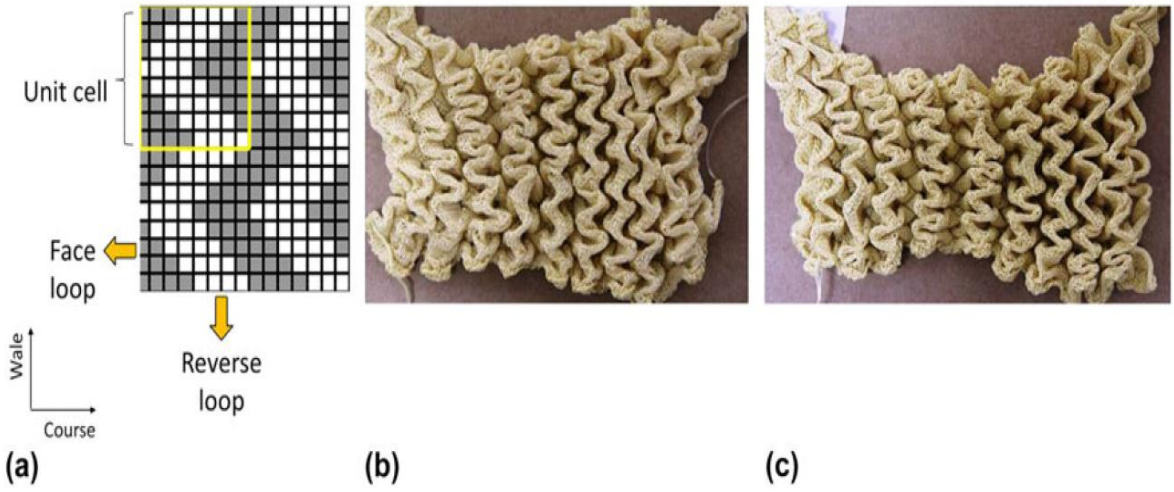

Fig (2.12): (a) Structural geometry of the knitted fabric and samples produced: (b) Hybrid structure, (c) 100% p-AR.

Fig (2.13): (a) Knitted fabrics impregnated in the resin placed on a raised and planar grid and (b) marked into specified dimensions (180 _ 40 mm).

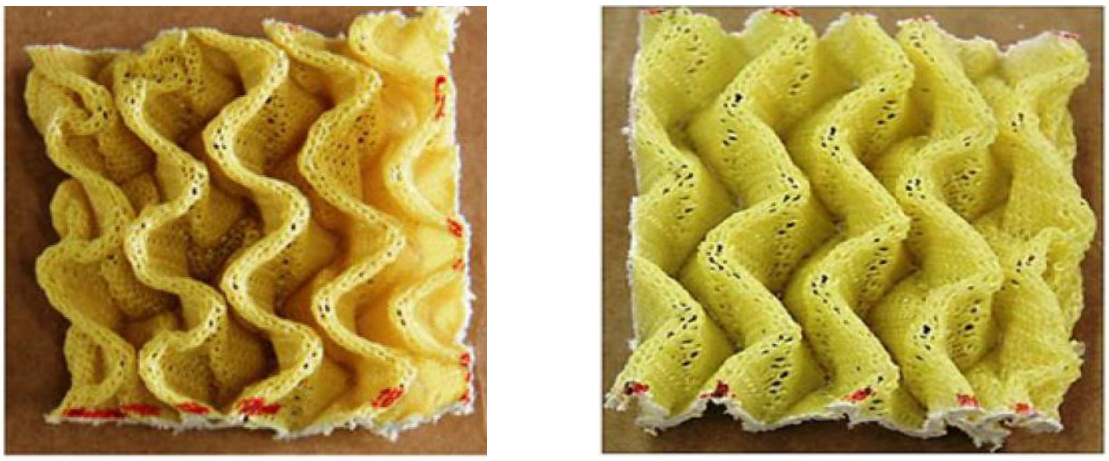

Fig (2.14): (a) Composite reinforced with p-AR and (d) hybrid auxetic knitted structure using epoxy resin.

Hu, H they studied using of weft-knitting technology to fabricate negative Poisson's ratio (NPR) knitted fabrics, which exhibit the unusual property of becoming wider when stretched. Based on a geometrical analysis of a three-dimensional NPR structure, a new kind of NPR weft-knitted fabric was firstly designed and fabricated on a computerized flat-knitting machine. Then the NPR values of these fabrics were evaluated and compared with those from the theoretical calculations. The results showed that all knitted fabrics have the NPR effect, which decreases with increased strain in the course direction. The results also showed that the main affecting structural parameter is the NPR (Hu, 2016).

Wang, X.-T., et al., designed an analytical model of a 3D re-entrant auxetic cellular structure that has been established based on energy method. Analytical solutions for the modulus and Poisson's ratios of the cellular structure in all principal directions were deduced. The results showed that when the struts are slender enough, the bending of the struts play decisive role on the deformation of the structure and other mechanisms can be ignored (Wang et al., 2017).

Ren, X., et al., studied a simple geometrical shape for achieving 3D auxetic behavior. The unit cell of the proposed 3D design is composed of a solid sphere and three cuboids. Two representative models are investigated both numerically and experimentally. The results indicate that the designed material with thick connecting bars did not exhibit auxetic behavior while the one with slender connecting bars did. show in fig (2.15) (Ren et al., 2018).

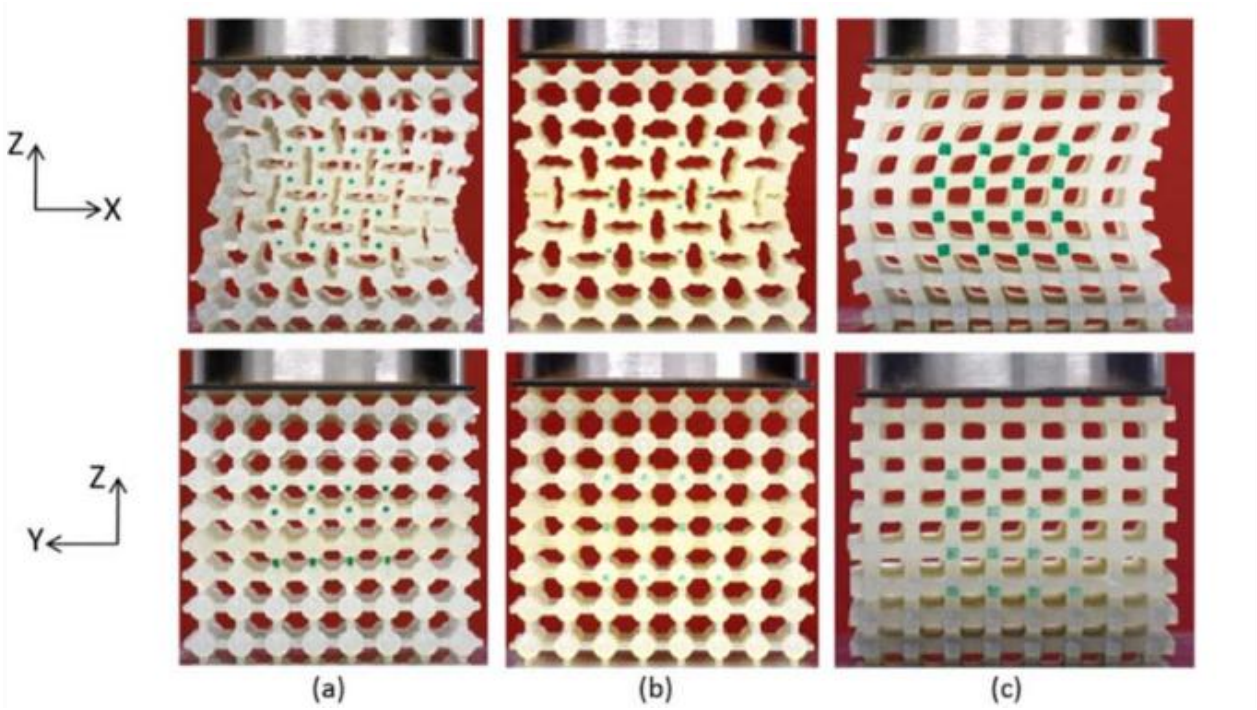

Fig (2.15) The deformation patterns of the three printed models in two lateral directions: (a) model with the SUC printed using insoluble supporting material; (b) model with the SUC printed using soluble supporting material; (c) model with the TUC printed using insoluble supporting material.

CHAPTER THREE

MATREIAL AND METHOD

3.1 Introduction:

This chapter focuses on the auxetic geometry design and the manufacturing process of the NPR weft knitted fabrics composite.

3.2 Material:

Textile reinforcements are produced using high performance fibers; these yarns have superior mechanical behavior that can meet the specific demands of composite applications. In this article's the PP yarn is used.

3.2.1 Polypropylenes yarn (PP):

PP yarn was used, due to easy to use in the knitting process, ductility, and the mechanical properties good.

The PP yarn was selected to be the reinforcement, due to availability in Sudan.

Knitted fabrics (knits fisherman's rib) were produced from 100 Tex, 72 monofilaments high tenacity PP yarns. PP yarn was supplied by Guangzhou Lanjing Chemical Fiber Co., Ltd.

3.3 Fabric Knitted structures:

Auxetic weft-knitted textile structures were manufactured on flat knitting machine (Passap Deumatic 80), using a 2-cam system with a pattern based on a (rib knitting) structure on the face and back loops, knit fabric structure was produced using 120 needles (60 in front-60 at back and 5 per/inch), as shown in Fig (3.1). The equipment allows controlling the needle selection, cam setting, and supporting the production of specimen structures.

Three different loop lengths knitted fabric were produced as illustrated in Fig (3.2).Loop length is the fundamental unit of weft knitted structure. Stitch/loop length is the fundamental unit which controls all the properties of weft knitted fabrics.(Evans et al., 1991)

The knits fisherman's rib was produced using a design of tuck loops length for the three different loop length (3, 4, 5), as it depicted in Fig (3.3) and (3.4).

Apassap knitting machine was used to produce fisherman's rib fabric.

Characteristics of rib:

- Appearance of face and back are identical.
- Fabric widthwise extension is approx twice.
- Fabric thickness is twice.
- Fabric dose not curl at the edges .

Effect of tuck stische:

- Fabric with tuck stitch is thicker than knit stitch.
- The structure with tuck stitch is wider.
- More open and porous (link).

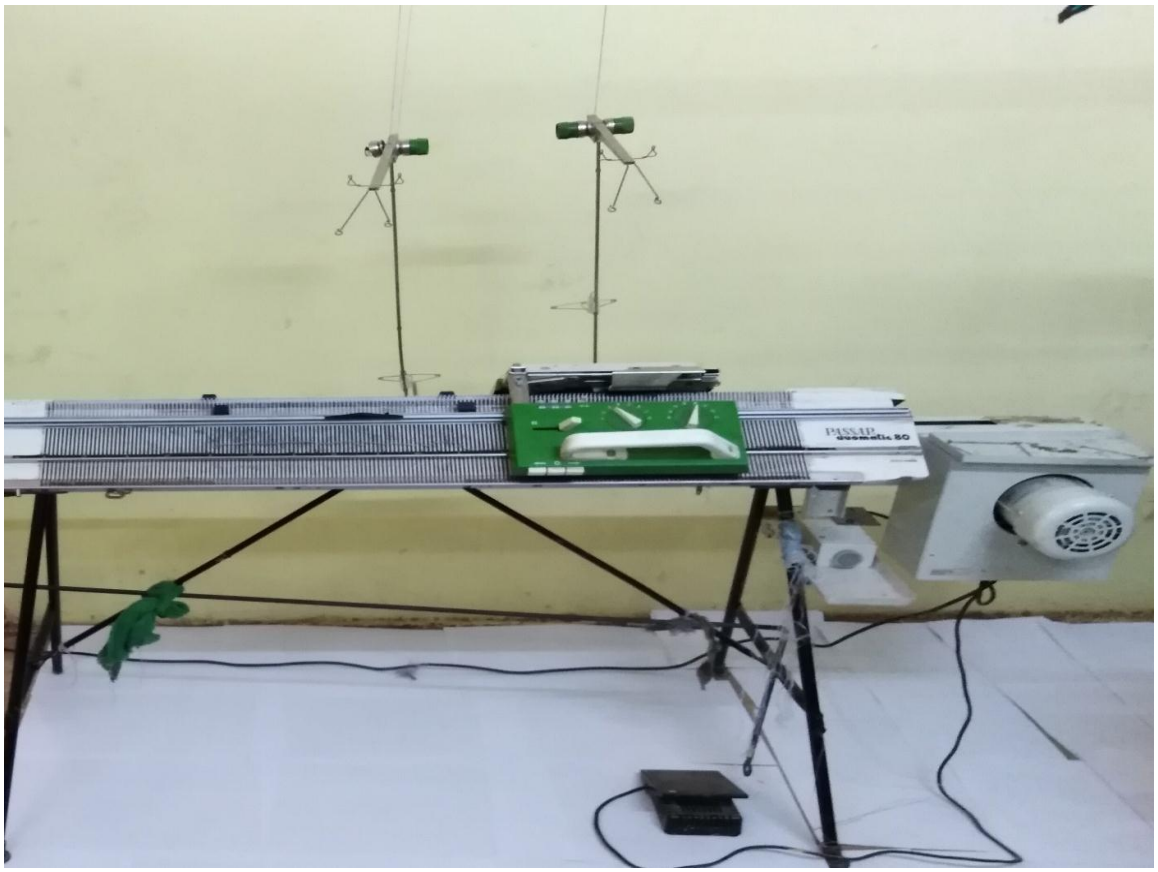

Fig (3.1): Passap Deumatic 80.

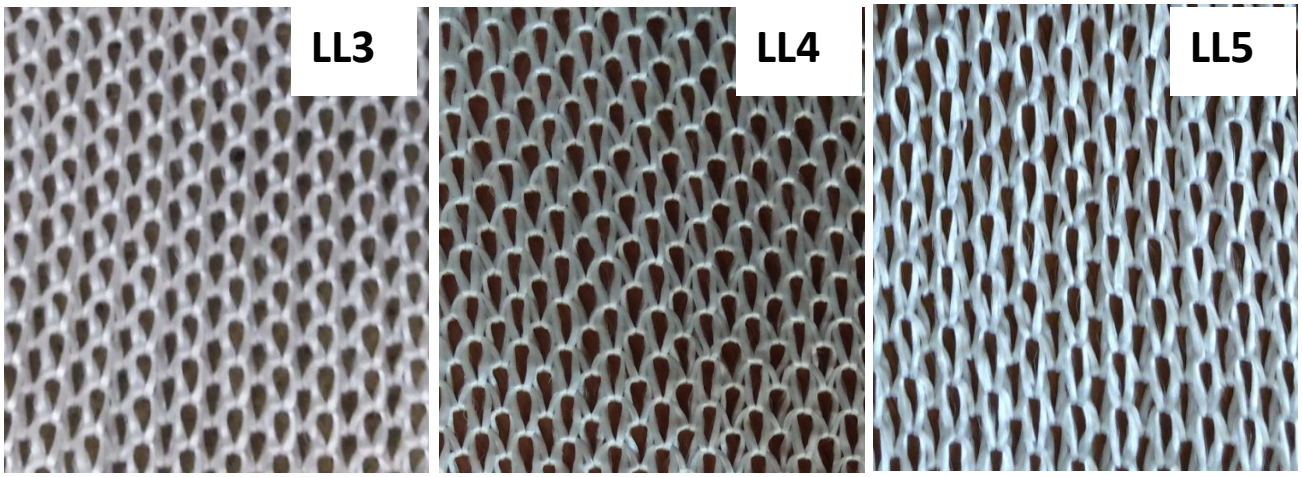

Fig (3.2): Three different loop lengths (LL)

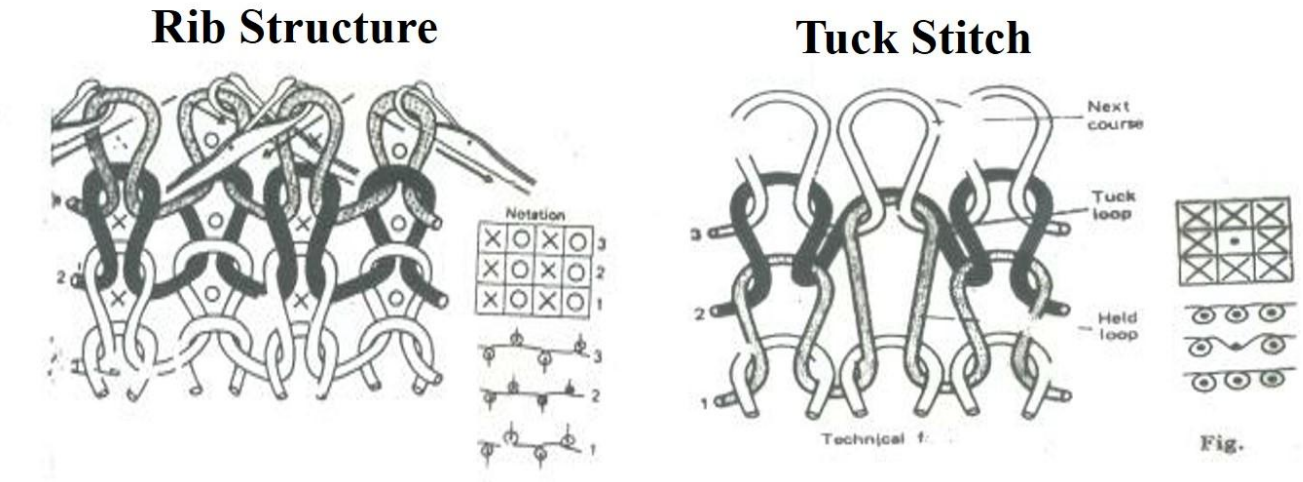

Fig(3.3): Structure of rib and tuck of knitted fabric(link)

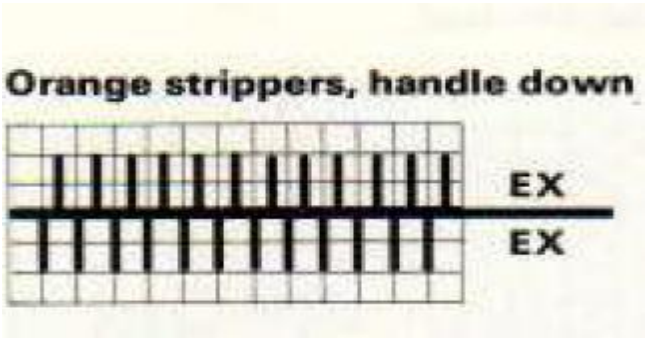

Fig (3.4): Knitted with all needles on both beds.
Fisherman's rib look the same on both sides.

3.4 Poisson's Ratio Evaluation:

Negative Poisson's ratio (NPR) are different from most conventional materials. They exhibit the veryunusual property of becoming wider when stretched and narrower when compressed (Evans et al., 1991).

In the literature, it is possible to find different ways to evaluate the deformation of auxetic specimens produced from knitted fabrics.

For the evaluation of NPR of the knitted structures, the specimens were clamped at their two ends in the testing device and extended manually along the course direction .The distance between the reference points along the course and wale

directions was 80mm and the change was observed in the specimen form as Shown in Fig (3.5).

The strains in the wale and course direction were calculated the following equations Eq (1,2)was used(Steffens et al., 2017).

$$\epsilon_x = {}^{\Delta L}/_{L} \quad \ldots\ldots\ldots\ldots\ldots\ldots (1) \quad \epsilon_y = {}^{\Delta W}/_{W} \quad \ldots\ldots\ldots\ldots\ldots\ldots\ldots\ldots (2)$$

Where is: ϵ_x is axial strain, ϵ_y is transverse strain.

L is length, W is width.

ΔL is length change in x direction , ΔW width change in y direction.

The values of ϵ_x and ϵ_y were determined by using Eq 1. The Poisson's ratio iscalculated through the relation between the strain in the transverse direction and the strain in the longitudinal direction using Eq (3) (Steffens et al., 2017).

$$v_{xy} = -\epsilon_y/\epsilon_x \quad \ldots\ldots\ldots\ldots\ldots\ldots (3)$$

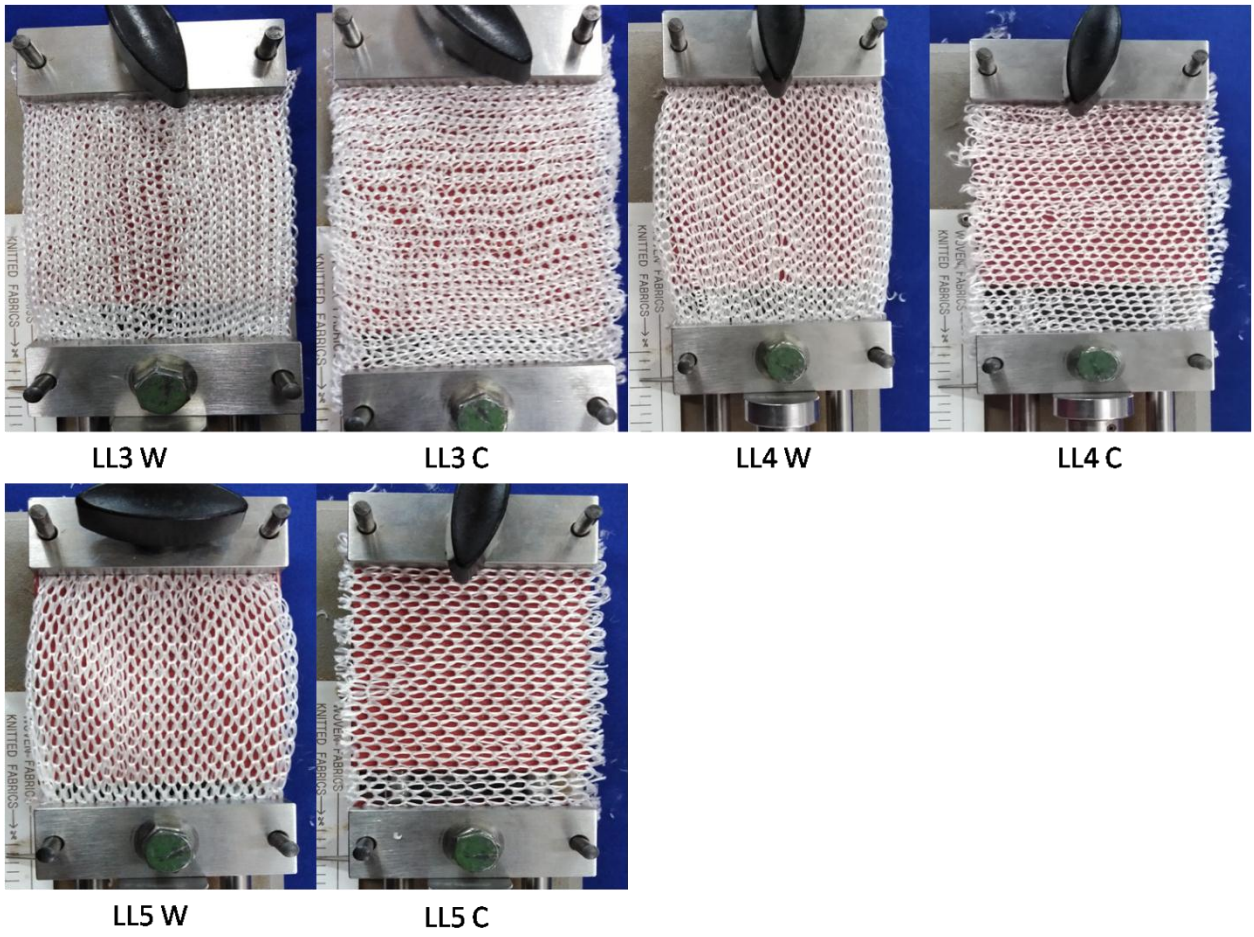

Fig (3.5): NPR for three different loop lengths (LL3, LL4, LL5).

3.5 Matrix (Resin):

The primary functions of the resin are to transfer stress between the reinforcing fibers, act as a glue to hold the fibers together, and protect the fibers from mechanical and environmental damage. Resins used in reinforced polymer composites are either thermoplastic or thermoset (Jawaid and Khalil, 2011).

3.5.1 Epoxy Resin:

In this work, thermoset epoxy resin has been chosen due to its exceptional combination of properties such as excellent toughness, adhesion, thermal, and chemical resistance(Risteski et al., 2017).

The resin was placed in the oven for half an hour at 60 C^{o} to get rid of the bubbles, as shown Fig (3.6).

Fig(3.6):Treatment of resin in 60c^{o} (miniature pressure and temperature).

3.5.2 Specifications of epoxy resin:

The Specifications of epoxy resin illustrate in Table (3.1).

Table (3.1)**:** main specifications of epoxy resin system**:**

Type	**Ingredient**	**Viscosity(room temperature) Mpa.s**	**Epoxy value Eq/100g**	**Density g/cm^3**	**Ratio of Epoxy:harder**
JC02A	Epoxy resin	1000-3000	0.50-0.53	1.12-1.14	1:0.8
JC02B	Modified anhydride	30-50	-	1.20-1.25	

3.6 Composites Manufacture Process:

3.6.1 Resin Transfer Molding (RTM):

Three different samples were manufactured based on the loop length using (RTM). The mold is then closed and a liquid thermoset resin is injected (Hammami et al.,

1998). Fabrics are laid up as a dry stack of materials. These fabrics are sometimes pre-pressed to the mold shape, and held together by a binder. These 'preforms' are then more easily laid into the mold tool. A second mold tool is then clamped over the first, and resin is injected into the cavity. Vacuum can also be applied to the mold cavity to assist resin in being drawn into the fabrics. This is known as Vacuum Assisted Resin Injection (VARI). Once all the fabric is wet out, the resin inlets are closed, and the laminate is allowed to cure. Both injection and cure can take place at either ambient or elevated temperature as shown in Fig(3.7) (Stark et al., 1990).

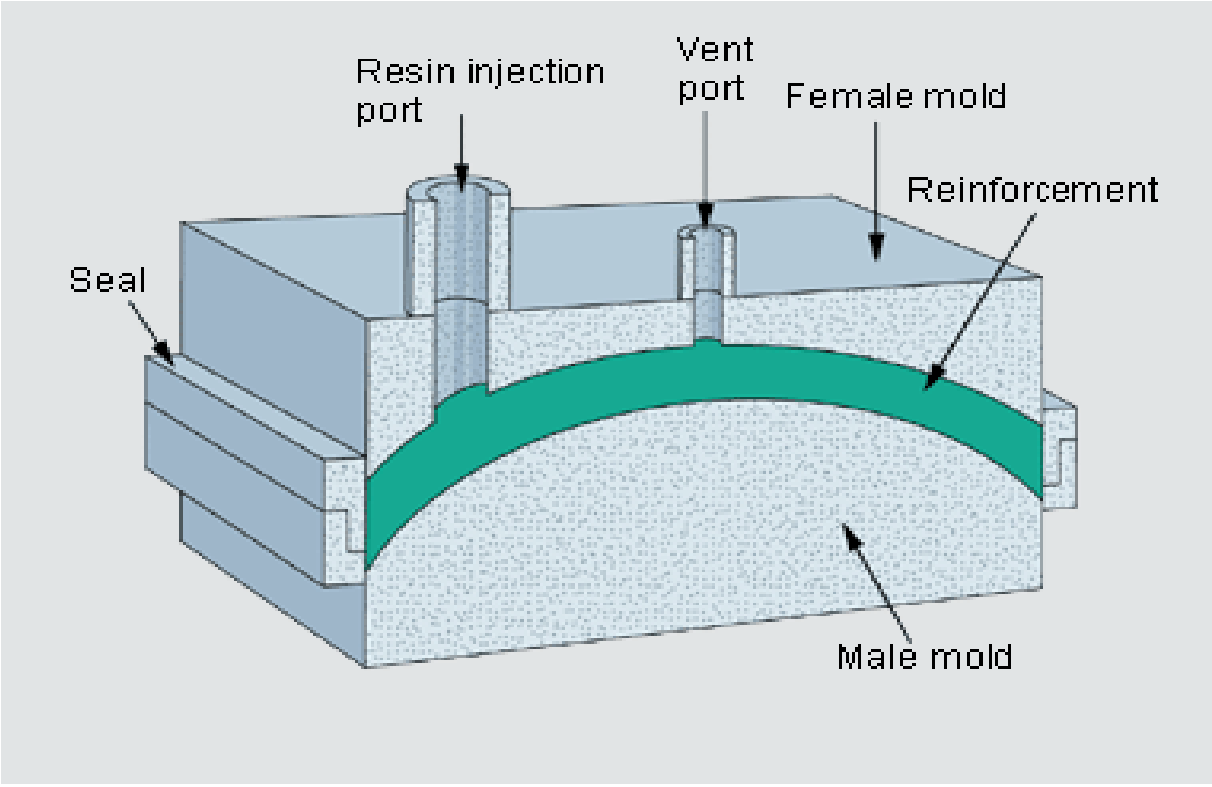

Fig (3.7): Resin Transfer Molding (RTM).

3.6.1.1 Process:

Resin Transfer Molding (RTM) the process which was used to manufacture the NPR Knitted composites with different loop length as shown in Fig (3.8). The process involves the use of a vacuum to facilitate resin (the epoxy and the harder

with ratio 1:0.8) flow into a fiber layup (8 layers with same direction) contained within a mold tool covered by a vacuum bag. After the impregnation with resin occurs the composite part is allowed to cure at the oven with the vacuum Pump pressure.

The sample was treated in the oven at 90° C for two hours. The temperature was increased to110° C for one hour, and 130° C for 4hoursand then allowed cooling down at room temperature for 8 hours, as shown Fig (3.9).

Fig (3.8): Resin Transfer Molding (RTM) process.

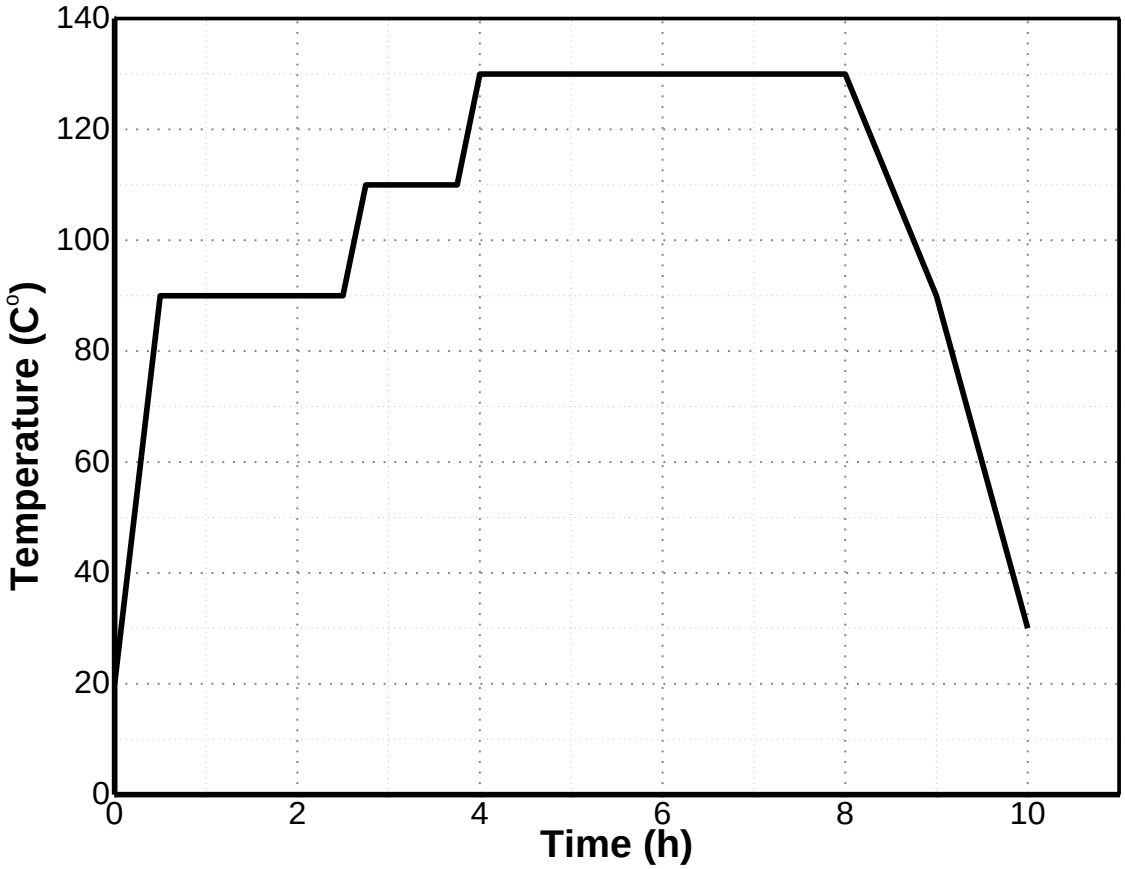

Fig (3.9): Temperature curing cycle for specimen fabrication.

3.7 Mechanical Testing:

In this research two testing's were used to study some mechanical properties for NPR knitted composite.

3.7.1 Tensile Test: Static tests

For the tensile tests, MTS 810 Material Test System-647 Hydraulic wedge Grip machine was used as shown in Fig (3.10). The applied velocity is 2 mm/min. Load–displacement plots were obtained for each test specimen, and three specimens of each type of NPR knitted composite are tested .

Fig (3.10)**:** MTS 810 Material Test System-647 Hydraulic wedge Grip machine.

3.7.2 Impact Test: Dynamic tests

This test method covers the damage resistance of polymer matrix composite laminate plates subjected to a drop- weight impact event.

When the impacted plate is tested in accordance with Test Method D 7137/D 7137M the overall test sequence is commonly referred to as the Compression after Impact (CAI) method as shown in Fig (3.11, and 3.12), the specimen dimensions cut by water saw are listed in Table (3.2).

The damage resistance properties generated by this test method are highly dependent upon several factors, which include specimen geometry layup, impactor geometry, impactor mass, impact force, impact energy, and boundary conditions Thus results are generally not scalable to other configurations, and are particular to the combination of geometric and physical conditions tested .

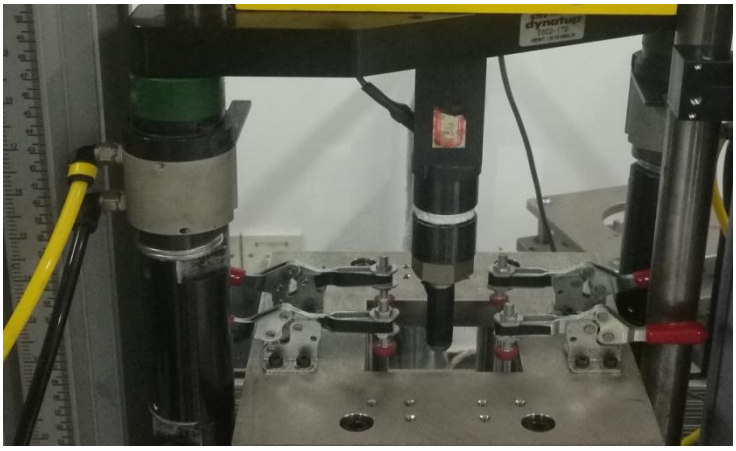

Fig (3.11) impact testing machine

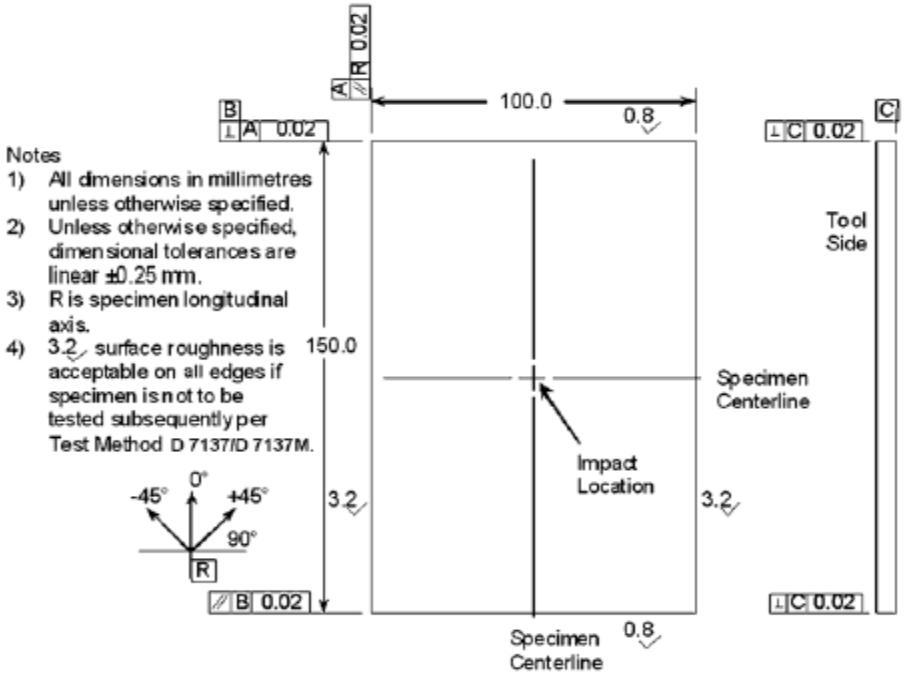

Fig (3.12): impact testing specimen dimensions

3.7.3 Preparation of Composite Specimen:

Table (3.2)**:** Dimensions of tests specimen:

Specimen Types and Specifications		
Unit	**Tensile Test**	**Impact Test**
Length (mm)	250	150
Width(mm)	25	100
Thickness (mm)	7	7

Fig (3.13): Specimen preparation for tensile test.

Fig (3.14): Specimen preparation for impact drop weight.

CHAPTER FOUR
RESULTS AND DISCUSSION

4.1 Evaluation of the Negative Poisson's ratio:

The strain in the longitudinal and transverse direction is inversely and directly proportionate with the loop length, respectively. Due to the negative Poisson ratio knitted fabric.

The shorter loop length, need longer elongation until a significant change in the transfer direction occurs as shown in Tables (4.1, 4.2).

Table (4.1)**:** The change in length and width of the three loop lengths in the wale:

L.L	L	ΔL	W	ΔW	$\in_x$	$\in_y$
L.L 3	8	+ 0.8	8	0	0.1	0
L.L 4	8	+ 1.5	8	+ 0.5	0.187	0.0620
L.L 5	8	+ 1.5	8	+ 0.7	0.187	0.087

Table (4.2)**:** The change in length and width of the three loop lengths in the course:

L.L	L	ΔL	W	ΔW	$\in_x$	$\in_y$
L.L 3	8	+ 2.6	8	+ 0.2	0.325	0.025
L.L 4	8	+ 2.0	8	+ 0.3	0.25	0.0375
L.L 5	8	+ 1	8	+ 0.4	0.125	0.05

4.2 Negative Poisson ratio:

Table (4.3) illustrated the NPR values for the wale and course direction, which show the auxetic behavior of the samples.

The highest values of NPR were found in the wale direction due to the amount of storage yarn in the unit area. The NPR was affected by the loop length, and maximum NPR at LL5.

These results refer to the type of the knitted fabric structure.

Table (4.3): The Negative Poisson ratio:

LL	NPR (wale direction)	NPR (course direction)
LL3	0	-0.076
LL4	-0.33	-0.2
LL5	-0.46	-0.4

4.3 Tensile test:

4.3.1 Load extension behavior:

The curves obtained in the tensile tests are shown in Fig (4.1 and 4.2).These curves were used to determine the behavior of the failure modes of NPR knitted fabric with different loop length.

All of these curves were similar in nature for the three loop length structures: LL3, LL4, and LL5. The curves can be divided into three regions, the first region, linear in appearance can explain the elastic deformation of the NPR weft knitted composites due to the composites sample carrying the load exerted, and the bonding was proper between the fiber and the matrix. The second region observes the oscillation form can explain the plastic deformation.

In the Third region the specimen continued to sustain the load but never exceeded the previous peak load as only the fiber were carrying the load, until the final failure occur. Except the LL3 was sudden failure after oscillation region.

It was observed the maximum load- extension occurred in the wale direction .due to the fabric applied in the loop direction.

In the course direction, it was observed the change in the extension of LL3 and LL4 was evident by 91%, and 50% from LL5, That can shown in fig (4.1).

(The loop length was directly proportionate with extension after applying a minimum load).

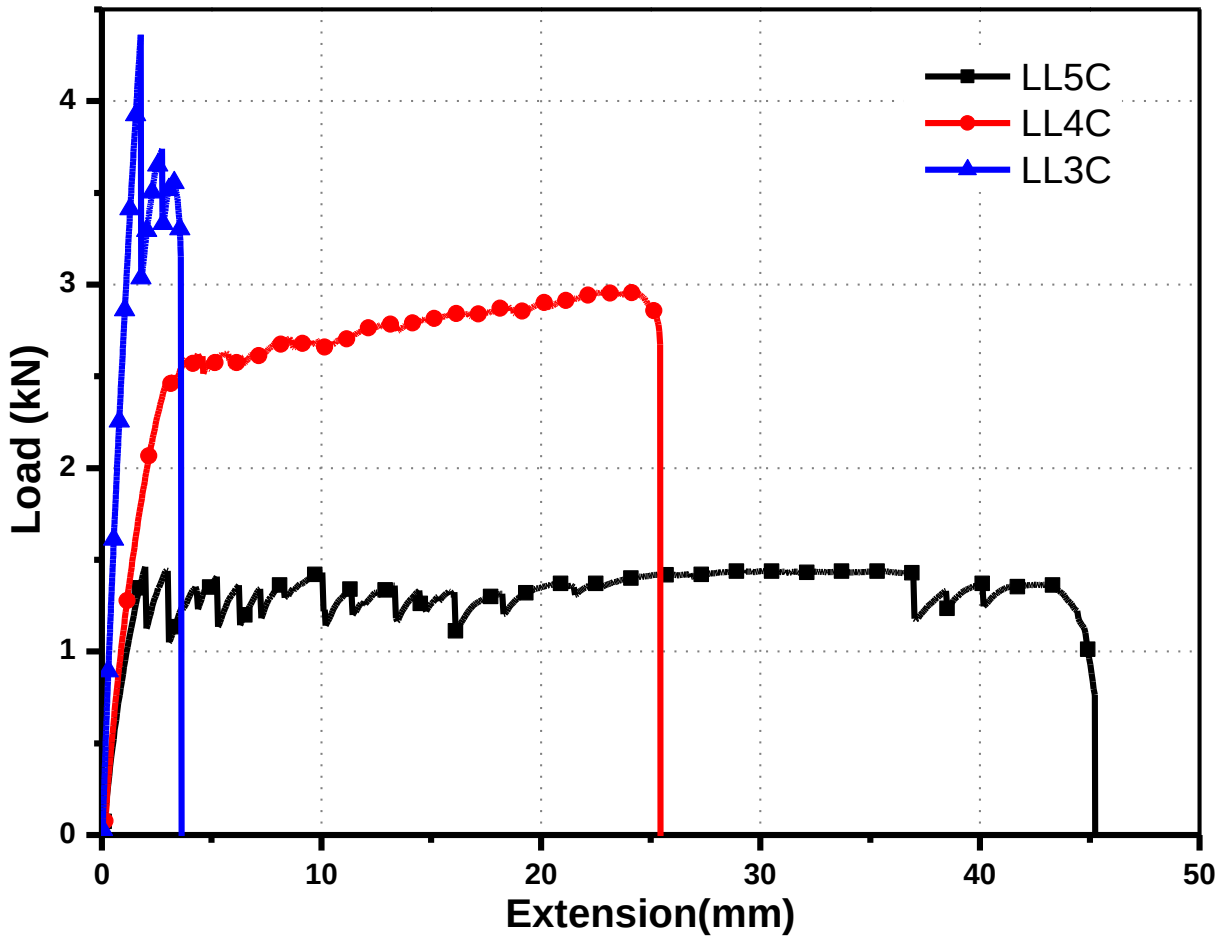

Fig (4.1): Load-extension curve of NPR knitting composite for three different loop lengths in course direction.

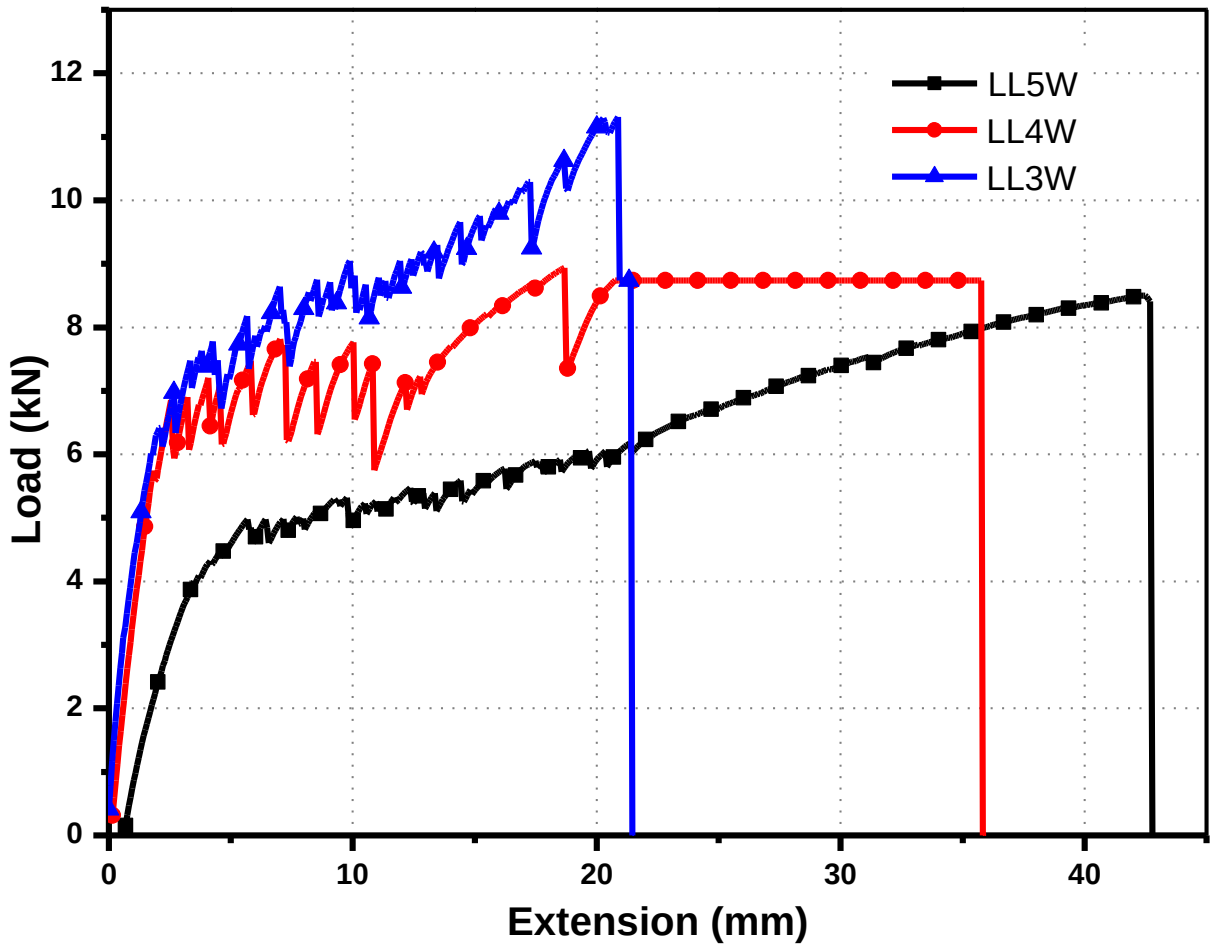

Fig (4.2): Load-extension curve of NPR knitting composite for three different loop lengths in wale direction.

Fig (4.3) compared the peak load for NPR knitted fabric composite at different loop length, the peak load of LL3 was the highest (4.5 KN and 11.2 KN), Due to shortness's of the loop lengths, and LL5 was lowest one (1.8 k N and 4.5 k N) in the course and wale direction respectively.

Fig (4.4) compared the extension for NPR knitting composite at different loop length, the extension of LL5 was highest (45 mm and 43mm), and LL3was lowest one (4 mm and 22 mm), in the course and wale direction respectively.

Observed the maximum extension of the three loop length occurs in the wale direction, especially for the LL5, due to the high NPR.

When compared between the course and wale direction from the different loop length from extension was found, whenever the length of the loop was decreased the difference was clear, except the LL5 Almost equal, due to the relaxation.

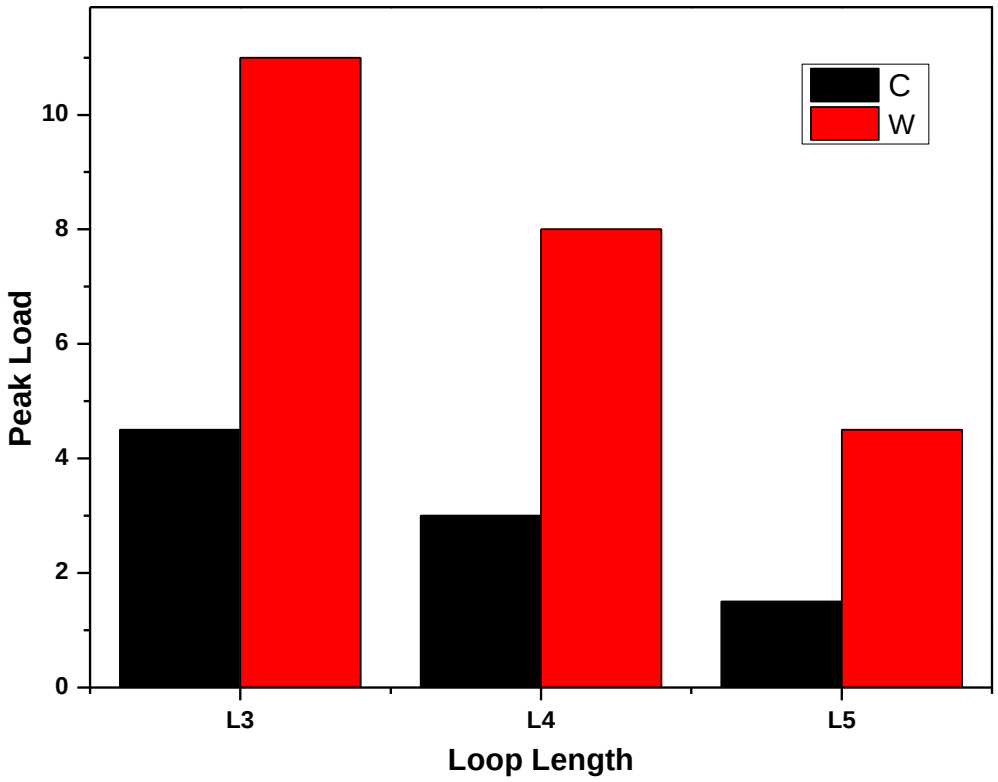

Fig (4.3): compared the peak load for NPR knitting composite at different loop lengths.

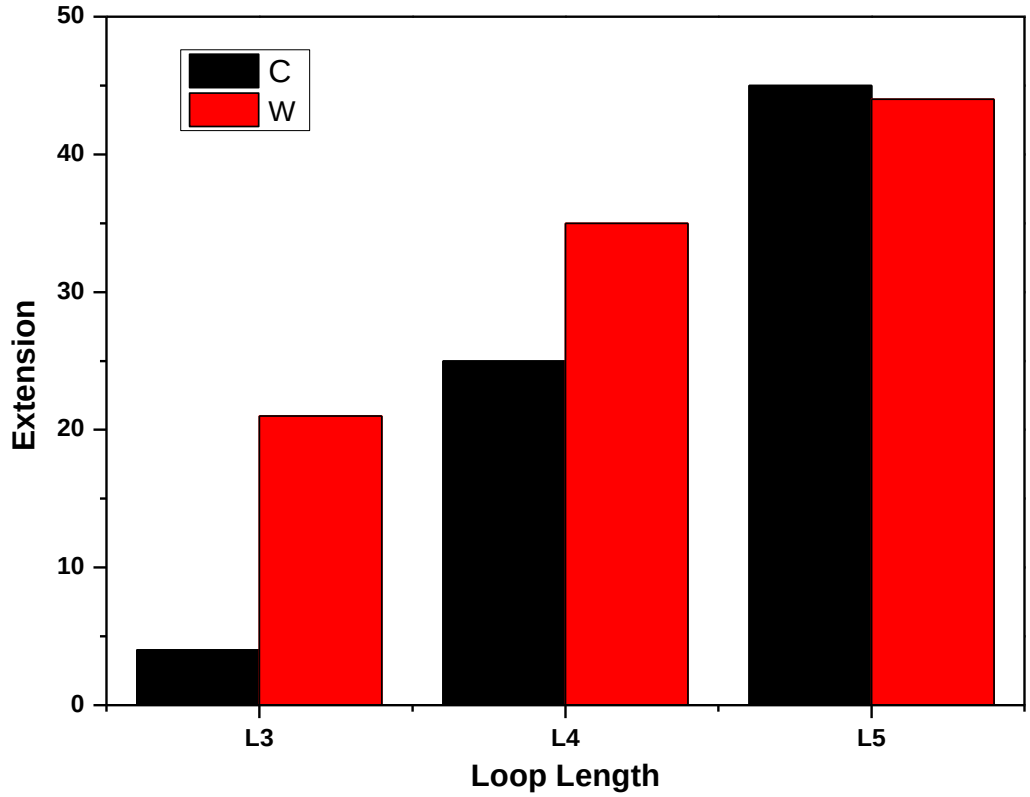

Fig (4.4): compared the extension for NPR knitting composite at different loop lengths.

4.3.2 Failure Modes:

Of ASTM D 3039 / D 3039M locate the sample failure. was selected a standard description using the three-part failure mode code. The failure observed for LL3 was similar Lateral Gage Middle (LGM), LL4 similar Angle Gage Middle (2) (AGM) and LL5 similar Angel Gage Middle (1) (AGM).From the three different loop lengths, the behavior were almost similar in the failure mode.

Specimens of the photograph were three different loop lengths. The improved interface as established earlier and this clearly affects the failure mode. Specimen LL3 has high tensile strength shows sudden break for the composite. Due to the composite has brittleness.

Specimen LL4 shows small fiber pull-out along the length of the composite, but no complete breakage for the fiber and breakage for the matrix.

Specimen (LL5) shows a high displacement; a failure is seen in the centre of the specimen length with some much localized micro-fibrillation, complete breakage for the fiber and crack for the matrix. Due to the ductility of the composite laminate and the failure was necked shape as shown in Fig (4.5).

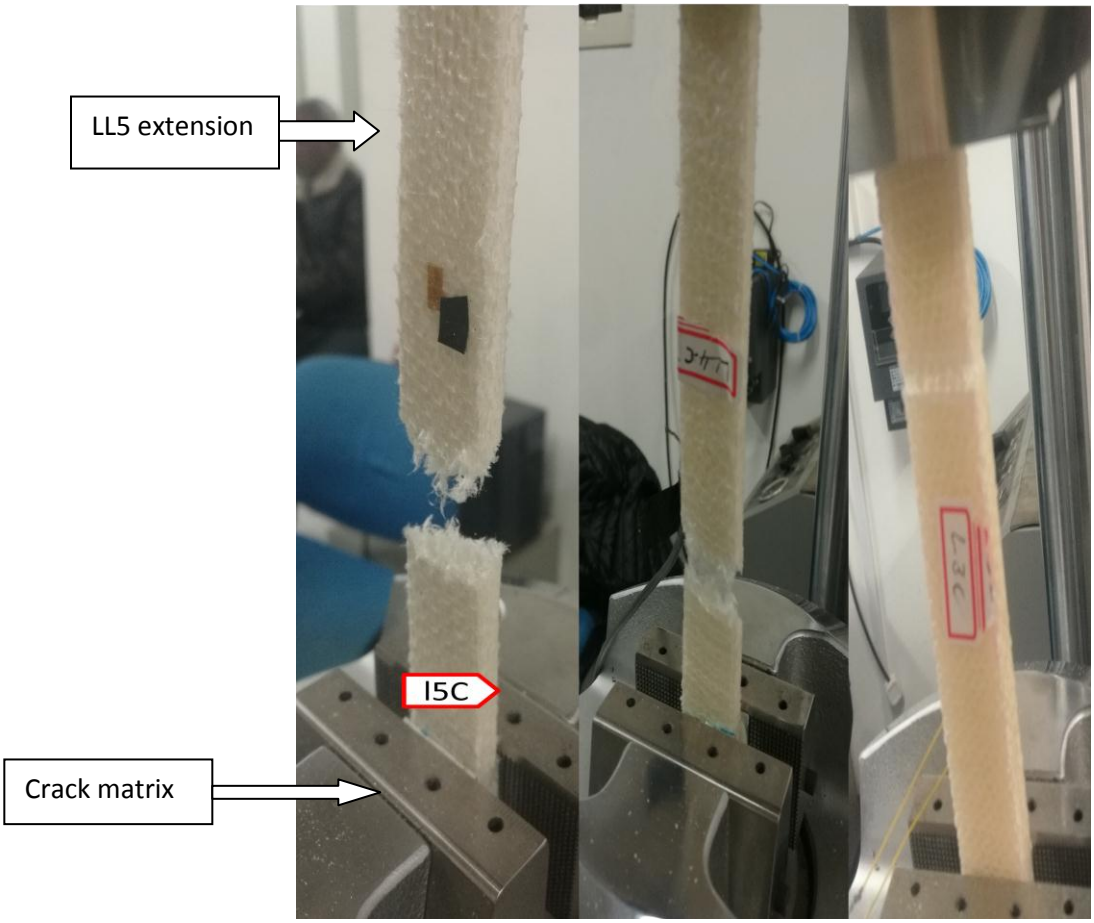

Fig (4.5): failure mode of tensile test.

4.4 Impact Drop Weight Test:

4.4.1 Load Displacement Behavior:

The load-displacement plots at different energy levels have been obtained by using the drop weight testing method in order to analyze the impact damage and failure model of the laminate composite with knitted fabric.

The load-displacement curves were showing same tendency, exhibiting a linear increase, with a small deformation. This behavior was attributed to the condition when the indenter comes in contact with the specimen, initiating delamination in the surface for specimen.

The peak load in the composite laminates slowly increased with the impact loading till a threshold was reached beyond which it either remained constant or reduced (when there is severe damage) with increasing energy.

The failure modes involved in impact damage under varied impact energies (10J, 20J, and 40J) of NPR weft knitting composite laminate.

The overall damage expansion of specimens after an impact event was evaluated by visual microscope. The failure modes involved in impact damage due to varied impact energies of the laminate composite structure of different loop length were characterized as combinations of matrix cracking, surface buckling, delamination, fiber fracture, and penetration. The impactor completely perforates the impacted surface, which usually interacted with each other. The delamination of composites under impact is caused by several complex interrelated processes (Lesser, 1997, Abrate, 2005, Liu, 1988).

Load–displacement curves for impact tests show oscillations before peak load for all samples at all energy levels, which may result from vibrations of the supports, some defects in composite laminates, to small delamination in the surface of laminates, and initiation of damage in the specimens. However, there were no oscillations observed after peak load for all samples at all energy levels, which may be a consequence of the different loop length and the difference NPR composite laminates. the load–displacement plots of NPR weft knitted composite laminate from different loop length (L3,L4,and LL5) at 10 J, 20 J, and 40 J impact energy as shown in Figs (4.6), (4.7), and (4.8).

The response of NPR weft knitted composite laminate to impact damage with different impact energy levels (10 J, 20 J, and 40 J) can be observed. The response was found that vary with peak loads, damage modes, curve types, absorbed energy, and displacement in composite specimens. These curves are characterized by an increase of the load up to a maximum load termed peak load, followed by a drop after the peak load, force oscillation, matrix crack, and delamination.

The maximum load of the LL5 fig (4.6) was around (1.3K N to 2.3KN) for the three impact energy level (10J, 20 J, and 40 J). While in the LL4 fig (4.7), for impact energy of 10 J, 20 J, and 40 J, peak forces were found it was vary from each other to be 2.3K N, 2.9K N, and 3.5K N, respectively. And in the LL3 fig (4.8), for impact energy of 10 J, 20 J, and 40 J, peak forces were found to be 2.3K N, 3.25K N, and 4K N, respectively.

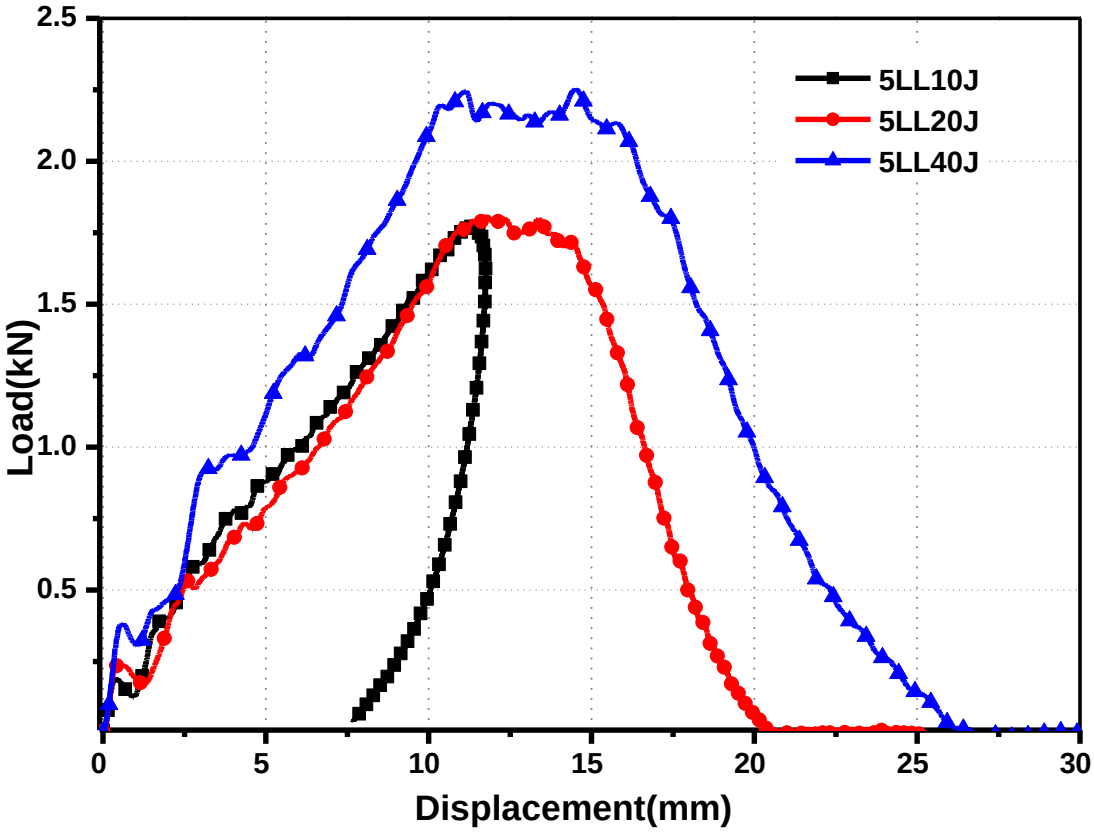

Fig (4.6): Load-displacement curves for impact tests of NPR knitting composite (LL5) with at 10, 20 and 40 J.

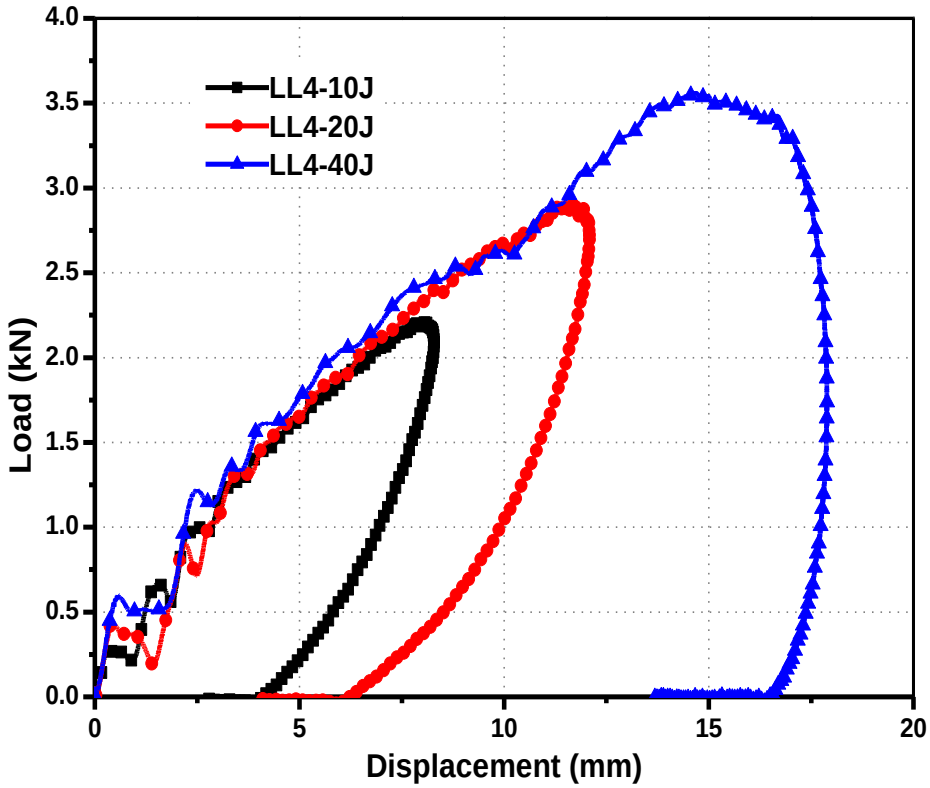

Fig (4.7): Load-displacement curves for impact tests of NPR knitted composite (LL4) at 10, 20 and 40 J.

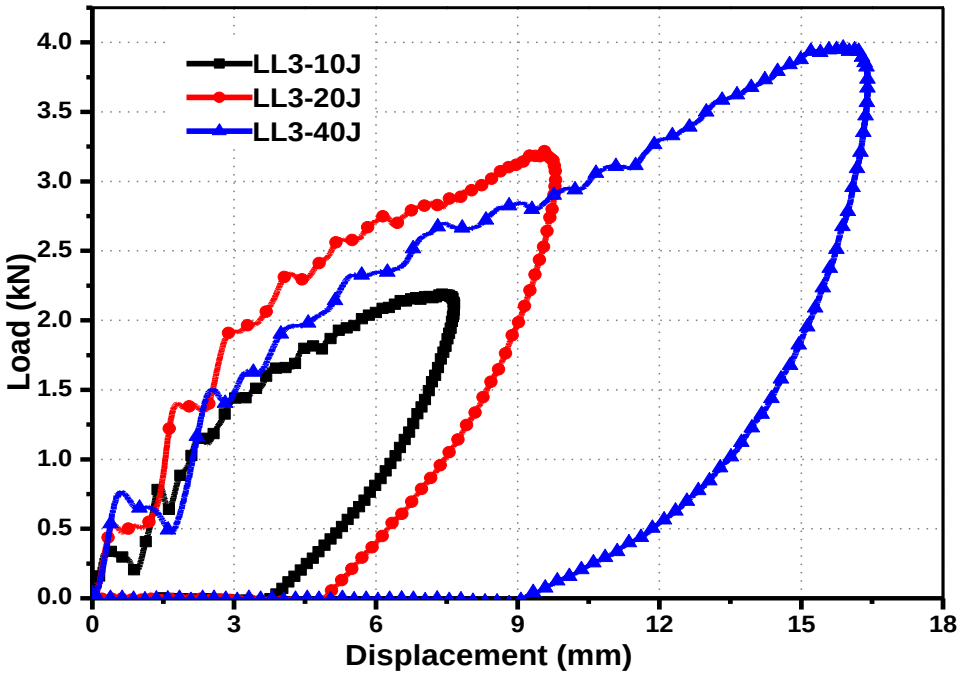

Fig (4.8): Load-displacement curves for impact tests of NPR knitted composite (LL3) at 10, 20 and 40 J.

Typical load–displacement curves of the laminate composite structure subjected to impact loading have shown three kinds of situations, including rebounding in 10 J case due to impact energy was not high enough to infiltrate full penetration and frictional force between the impactor and the composite plate. The rebounding case results in closed curves indicating the rebounding of the impactor from the specimen surface, Deformation in 20 J and delamnation in 40 J.

A higher ductility of the material would mean that most of the total energy is expanded in crack propagation (Hani et al., 2013). When the impact energy increases, the open-type curve bounds larger areas and displacement increases while rebounding sections become smaller. As the impact energy continues to increase, the curve type changes from the closed to the open type, Load–displacement curves, can be classified as, closed-type curves in of different loop length were observed in 10 J case in Fig (4.9), 20J (4.10) ,40J in Fig (4.11). Open-type curves were observed in 20 J and 40 J that could be as a result of variation in loop length, the critical point to carry additional load of composite, mechanical properties of laminate, and the amount of the total absorbed energy.

If the curve was an open type, the specimen is either deformation or delamnation by the impactor.

4.4.2 NPR effect on the impact test:

An increase in displacement was observed due to the increase in NPR's value. And it's all due to the direct effect of the loop length. The displacement was found to be increased with an increase in the impact energy levels .The variation of displacement from low- to high-impact energy was attributed to the penetration depth of the indenter.

In fig (4.6) the behaviour of the curve of impact tests was observed to be similar only for 20 J and 40 J impact energies, which could be attributed to the composite

laminates not being able to carry high loads, but the displacement was higher, due to the ductility of the composite laminate.

Figs (4.7, 4.8) illustrated the load-displacement of the LL4 and LL3 was observed that different behaviour of the curve for 20J and 40J. This could be attributed to the fact that until 20 J the composite laminate has resistance to impact damage. This explains the variation of high load of the composite laminates in two levels of the impact energy .The maximum load was observed in LL3 (4.0KN), Due to high fiber volume fraction that lead to the composite has brittleness.

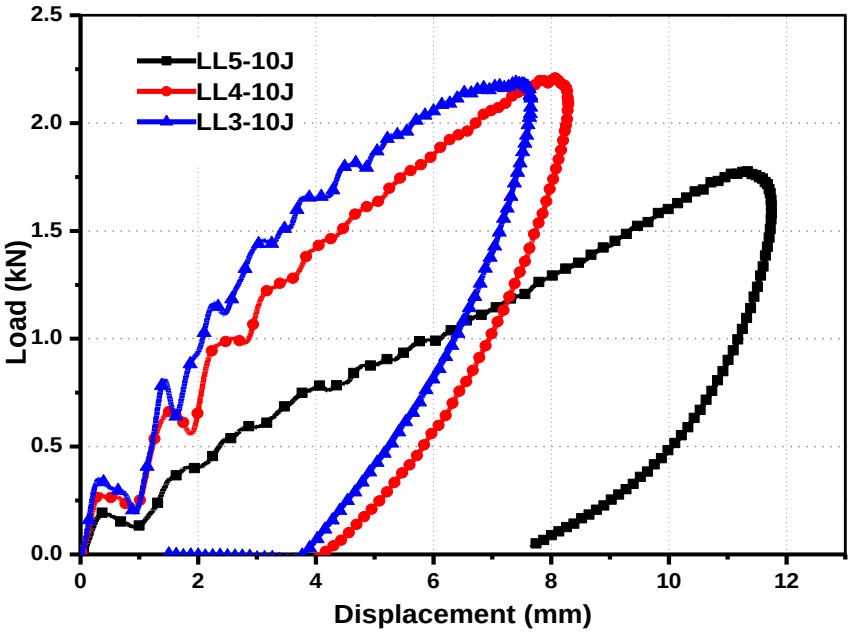

Fig (4.9): Load-displacement curves for impact tests of NPR knitted composites from different loop lengths at 10J.

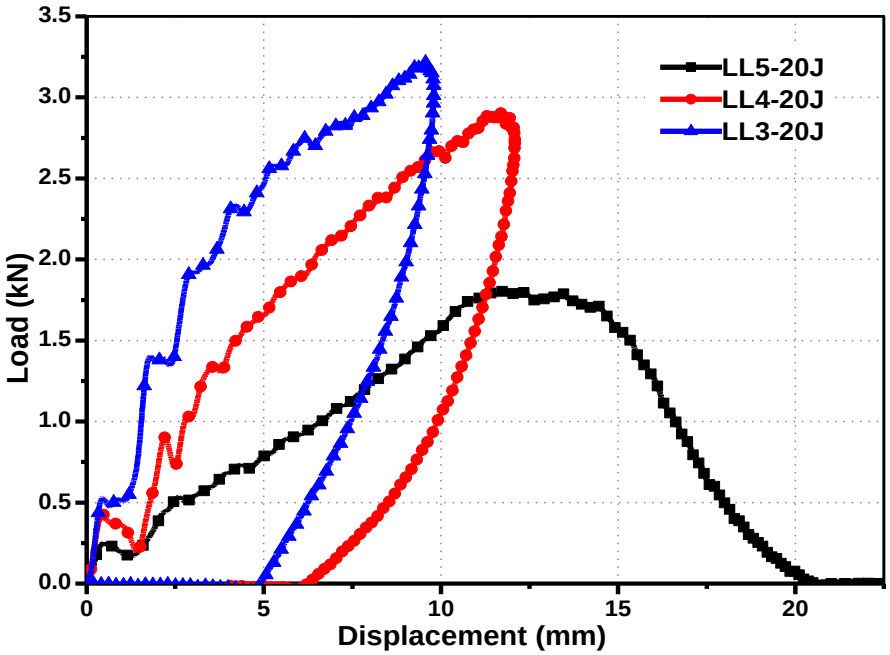

Fig (4.10): Load-displacement curves for impact tests of NPR knitted composites from different loop lengths at 20J.

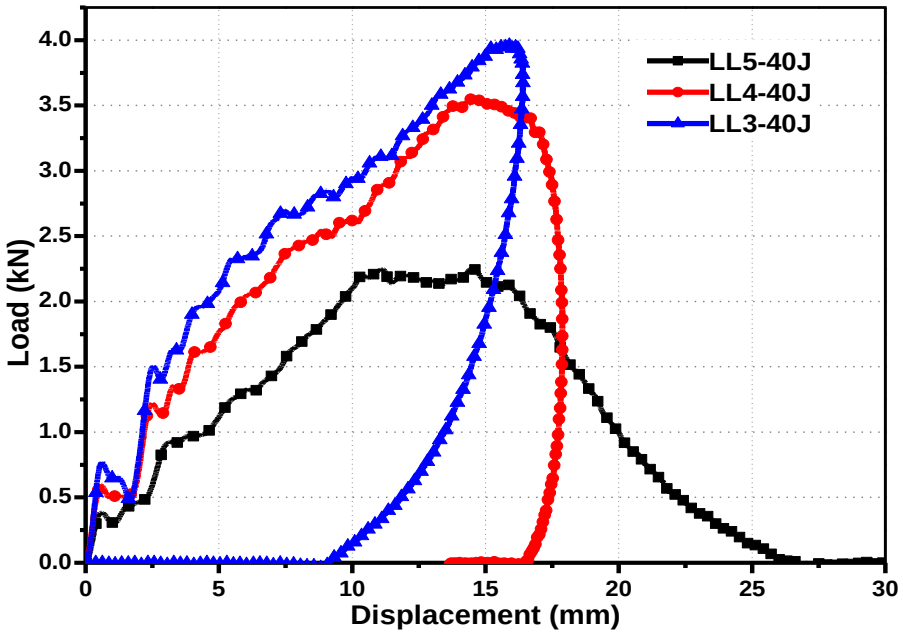

Fig (4.11): Load-displacement curves for impact tests of NPR knitted composites from different loop lengths at 40J.

4.4.3 Failure Modes:

Failure modes were studied under optical microscope at the impact location in Figs (4.12), (4.13), and (4.14).

All cracks propagate toward the compressive side of the specimen. However, Damage in the specimen can be classified into matrix cracking, with fiber breakage.

The impact energy was chosen to be 10 J, 20 J, and 40 J, for the LL3 at 10 J the form of damage small cracked in the matrix with small damage in the fiber, the first indication of damage was observed at 20J, and the damage form was cracked in the matrix with damage in the fiber, A second index of damage was observed in 40 J, and the damage form was fiber breakage with matrix crack in Fig (4.12). for the LL4 at 10J the damage was cracked in the matrix with small damage in the fiber, the damage was observed at 20J, and the damage form was cracked in the matrix and fiber breakage, for 40J there was significant damage (fiber pull-out and the composite crack) shown in Fig (4.13), and LL5 observed at 10J the damage form was cracked in the matrix with damage in the fiber, for 20J,and 40J there was significant damage (fiber pull-out and the composite crack),and the sample was failure illustrated in Fig (4.14).

4.4.4 Damage Area:

The overall damage expansion of specimens after an impact event was evaluated by visual microscope. The failure modes involved in impact damage due to varied impact energies of the laminate composite structure of different loop length were characterized as combinations of matrix cracking, surface buckling, delamination, and fiber fracture. As the impact energy is increased, the area of composite deformation increased.

The smallest area of damage shown in LL3 at 10j, and that the biggest area of damage was observed in LL5 at 40 j, illustrated in Figs (4.12) and (4.14)

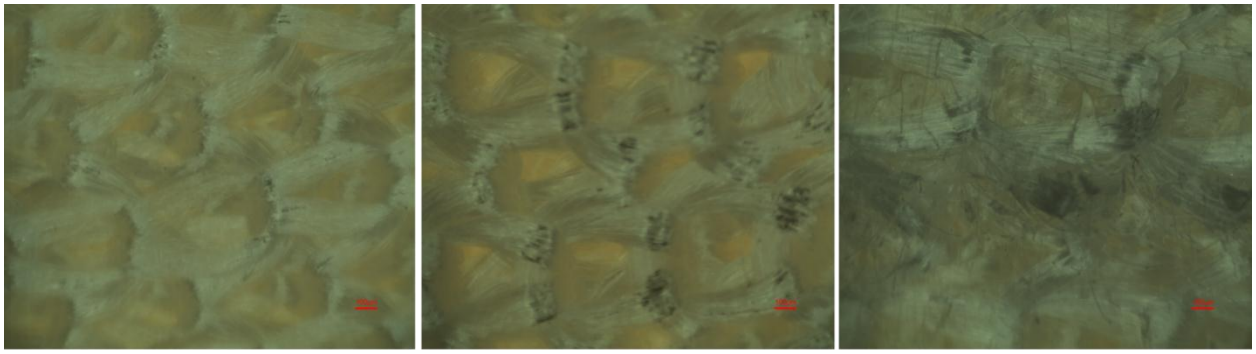

Fig (4.12): The surfaces of samples with LL3 under 10, 20 and 40 J.

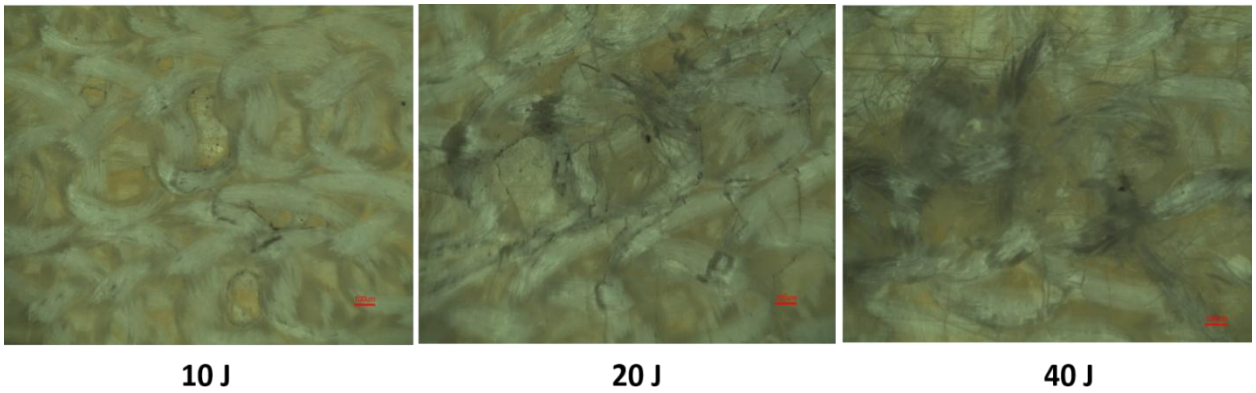

Fig (4.13): The surfaces of samples with LL4 under 10, 20 and 40 J.

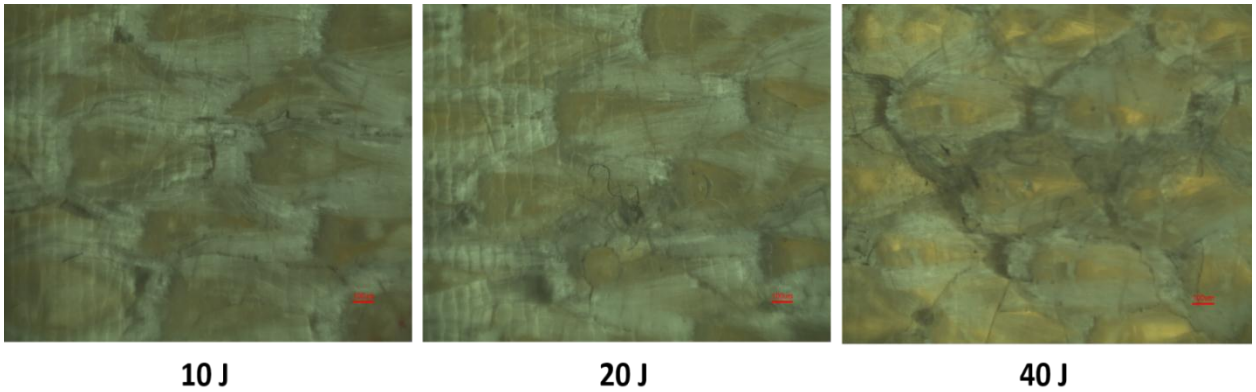

Fig (4.14): The surfaces of samples with LL5 under 10, 20 and 40 J.

CHAPTER FIVE
CONCLUSION AND RECOMMENDATIONS

5-1 Conclusion:

In this study, composites reinforced with NPR weft knitted fabric have been developed using polypropylene yarn and manufactured by Resin Transfer Molding (RTM).The auxetic behavior transfer from the reinforcing fabric to the composite was thoroughly investigated for three different loop lengths by evaluating the Poisson's coefficient. The results obtained show that, although the auxetic behavior decreases, it is still maintained in the produced composites.

In the selection of materials, found that the NPR composite materials have good characteristics of high tensile and impact resistance, ductility, light weight, flexibility.

The used of high-ductile yarn, such as PP in the production of the NPR weft-knitted fabric, result strong improvement of NPR composites.

For a given fabric structure, different NPR values can be obtained by varying the loop length. Among the different loop length the highest NPR value was observed to be at LL5.

The NPR was affected by the loop length, when the loop length increase the NPR increase (the loop length was directly proportionate with NPR).

When comparing between the course and wale direction from the different loop lengths the extension of the loop length decreased the difference was clear, except the LL5 Almost equal, due to the relaxation.

The failure mode of tensile test showed that LL3 sample is better than LL5 in load bearing and conversely in extension.

In dynamic impact drop weight test all samples absorbed all exposed energy.

The LL3 was absorbing energy up to 40 J and LL5 absorbed about 20 J.

Optical Microscopic images showed that the impact damage size estimated by visual inspection was much more extensive in all samples.

The smallest area of damage shown in LL3 and that the biggest area of damage was observed in LL5.

5-2 Recommendations:

NPR weft knitting Composite has high impact strength and low cost so we recommend to:

- Concern for the manufacture of NPR weft knitting Composite for their good properties, easy of manufacturing and low cost.
- The NPR weft knitting composite takes brittleness behavior.
- Use of natural fibers available in Sudan as a NPR reinforced composite, for good properties and lowest cost, and providing modern machines (3D machine).
- To continue the future research to learn more about the mechanical properties of NPR knitting composite , its behavior and study all the factors affecting.
- Be careful about conditions for manufacturing laminate composite and about the degree of temperature, uniform distribution of the resin in the sample and the bonding between the overall layers of the composite. To avoid manufacture faults. Because every step in the manufacturing process affects the final mechanical properties of the composite.
- The NPR weft knitting composite can be used in bulletproof vests, aerospace, automobile's Bumper, Defense, ball racket, table, chair, partition, and in all other areas where energy absorption is a key factor to be considered.

REFERENCES

. Available: http://sas-articles.blogspot.com/2010/04/characteristics-of-rib-fabric.html.

impact tests [Online]. Available: https://wenku.baidu.com/view/8b9ccd7f5acfa1c7aa00ccd6.html.

tensile tests [Online]. Available: https://wenku.baidu.com/view/04dd3f0af78a6529647d5322.html?re=view.

ABRATE, S. 2005. *Impact on composite structures*, Cambridge university press.

ALDERSON, A. & ALDERSON, K. 2005. Expanding materials and applications: exploiting auxetic textiles. *Technical textiles international*, 14**,** 29-34.

ALDERSON, A. & EVANS, K. E. 2002. Molecular origin of auxetic behavior in tetrahedral framework silicates. *Physical review letters*, 89**,** 225503.

ALDERSON, K., WEBBER, R. & EVANS, K. 2007. Microstructural evolution in the processing of auxetic microporous polymers. *physica status solidi (b)*, 244**,** 828-841.

ASSIDI, M. & GANGHOFFER, J.-F. 2012. Composites with auxetic inclusions showing both an auxetic behavior and enhancement of their mechanical properties. *Composite Structures*, 94**,** 2373-2382.

ATTARD, D. & GRIMA, J. N. 2008. Auxetic behaviour from rotating rhombi. *physica status solidi (b)*, 245**,** 2395-2404.

ATTARD, D., MANICARO, E. & GRIMA, J. N. 2009. On rotating rigid parallelograms and their potential for exhibiting auxetic behaviour. *physica status solidi (b)*, 246**,** 2033-2044.

BERTOLDI, K., REIS, P. M., WILLSHAW, S. & MULLIN, T. 2010. Negative Poisson's ratio behavior induced by an elastic instability. *Adv Mater*, 22**,** 361-6.

CABRAS, L. & BRUN, M. Auxetic two-dimensional lattices with Poisson's ratio arbitrarily close to− 1. Proceedings of the Royal Society of London A: Mathematical, Physical and Engineering Sciences, 2014. The Royal Society, 20140538.

CARNEIRO, V., MEIRELES, J. & PUGA, H. 2013a. Auxetic materials—A review. *Materials Science-Poland*, 31**,** 561-571.

CARNEIRO, V. H., MEIRELES, J. & PUGA, H. 2013b. Auxetic materials—A review. *Materials Science-Poland*, 31**,** 561-571.

DANIEL, I. M., ISHAI, O., DANIEL, I. M. & DANIEL, I. 1994. *Engineering mechanics of composite materials*, Oxford university press New York.

DARJA, R., TATJANA, R. & ALENKA, P.-Č. 2014. Auxetic textiles. *Acta Chimica Slovenica*, 60**,** 715-723.

EVANS, K. & ALDERSON, K. 2000a. Auxetic materials: the positive side of being negative. *Engineering Science & Education Journal,* 9**,** 148-154.

EVANS, K. E. & ALDERSON, A. 2000b. Auxetic materials: functional materials and structures from lateral thinking! *Advanced materials,* 12**,** 617-628.

EVANS, K. E., NKANSAH, M., HUTCHINSON, I. & ROGERS, S. 1991. Molecular network design. *Nature,* 353**,** 124.

GE, Z. & HU, H. 2013. Innovative three-dimensional fabric structure with negative Poisson's ratio for composite reinforcement. *Textile Research Journal,* 83**,** 543-550.

GIBSON, R. F. 2011. *Principles of composite material mechanics*, CRC press.

GRIMA, J. N. 2010. Auxetic metamaterials. *Strasbourg, France*.

GRIMA, J. N. & EVANS, K. E. 2006. Auxetic behavior from rotating triangles. *Journal of materials science,* 41**,** 3193-3196.

GRIMA, J. N., GATT, R., ALDERSON, A. & EVANS, K. 2005. On the potential of connected stars as auxetic systems. *Molecular Simulation,* 31**,** 925-935.

GRIMA, J. N., ZAMMIT, V., GATT, R., ALDERSON, A. & EVANS, K. 2007. Auxetic behaviour from rotating semi-rigid units. *physica status solidi (b),* 244**,** 866-882.

GULHANE, S. S., RAHANGDALE, P. S., UBARHANDE, D. P. & INGOLE, M. S. 2014. A Review on Structure-Property Relationship of Knitted Composites. *International Journal of Research in Advent Technology,* 2**,** 208-210.

HAMMAMI, A., GAUVIN, R. & TROCHU, F. 1998. Modeling the edge effect in liquid composites molding. *Composites Part A: applied science and manufacturing,* 29**,** 603-609.

HANI, A., RASHID, A., SEANG, C. T., AHMAD, R. & MARIATTI, J. M. Impact and flexural properties of imbalance plain woven coir and kenaf composite. Applied Mechanics and Materials, 2013. Trans Tech Publ, 81-85.

HE, C., LIU, P., MCMULLAN, P. J. & GRIFFIN, A. C. 2005. Toward molecular auxetics: Main chain liquid crystalline polymers consisting of laterally attached para-quaterphenyls. *physica status solidi (b),* 242**,** 576-584.

HORROCKS, A. R. & ANAND, S. C. 2000. *Handbook of technical textiles*, Elsevier.

HU, H. 2016. Auxetic Textile Materials - A review. *Journal of Textile Engineering & Fashion Technology,* 1.

HU, H., WANG, Z. & LIU, S. 2011. Development of auxetic fabrics using flat knitting technology. *Textile Research Journal,* 81**,** 1493-1502.

HURSA, A., ROLICH, T. & RAŽIĆ, S. E. 2009. Determining pseudo Poisson's ratio of woven fabric with a digital image correlation method. *Textile research journal,* 79**,** 1588-1598.

JACOBS, M. & VAN DINGENEN, J. 2001. Ballistic protection mechanisms in personal armour. *Journal of materials science,* 36**,** 3137-3142.

JAWAID, M. & KHALIL, H. A. 2011. Cellulosic/synthetic fibre reinforced polymer hybrid composites: A review. *Carbohydrate polymers,* 86**,** 1-18.

LESSER, A. J. 1997. Effect of resin crosslink density on the impact damage resistance of laminated composites. *Polymer composites,* 18**,** 16-27.

LINK. *Effect of tuck stisches* [Online]. Available: https://webcache.googleusercontent.com/search?q=cache:IazZZN9QLH8J:https://textilestudycenter.com/tuck-stitch-formation-process/+&cd=6&hl=en&ct=clnk.

LIU, D. 1988. Impact-induced delamination—a view of bending stiffness mismatching. *Journal of composite materials,* 22**,** 674-692.

LIU, Q. 2006. Literature review: materials with negative Poisson's ratios and potential applications to aerospace and defence. DEFENCE SCIENCE AND TECHNOLOGY ORGANISATION VICTORIA (AUSTRALIA) AIR VEHICLES DIV.

LIU, Y. & HU, H. 2010. A review on auxetic structures and polymeric materials. *Scientific Research and Essays,* 5**,** 1052-1063.

LIU, Y., HU, H., LAM, J. K. & LIU, S. 2010. Negative Poisson's ratio weft-knitted fabrics. *Textile Research Journal,* 80**,** 856-863.

MILLER, W., HOOK, P., SMITH, C. W., WANG, X. & EVANS, K. E. 2009. The manufacture and characterisation of a novel, low modulus, negative Poisson's ratio composite. *Composites Science and Technology,* 69**,** 651-655.

MILTON, G. W. 1992. Composite materials with Poisson's ratios close to—1. *Journal of the Mechanics and Physics of Solids,* 40**,** 1105-1137.

N. GRIMA, J., GATT, R., ALDERSON, A. & E. EVANS, K. 2005. On the Auxetic Properties ofRotating Rectangles' with Different Connectivity. *Journal of the Physical Society of Japan,* 74**,** 2866-2867.

PICKLES, A., ALDERSON, K. & EVANS, K. 1996. The effects of powder morphology on the processing of auxetic polypropylene (PP of negative Poisson's ratio). *Polymer Engineering & Science,* 36**,** 636-642.

PRAWOTO, Y. 2012. Seeing auxetic materials from the mechanics point of view: a structural review on the negative Poisson's ratio. *Computational Materials Science,* 58**,** 140-153.

RANA, S. & FANGUEIRO, R. 2016. *Advanced composite materials for aerospace engineering: Processing, properties and applications*, Woodhead Publishing.

RAZ, S. 1987. *Warp knitting production*, Melliand.

RAZ, S. 1991. *Flat knitting: the new generation*, Meisenbach.

REN, X., SHEN, J., TRAN, P., NGO, T. D. & XIE, Y. M. 2018. Design and characterisation of a tuneable 3D buckling-induced auxetic metamaterial. *Materials & Design,* 139**,** 336-342.

RISTESKI, S., ZHEZHOVA, S. & SREBRENKOSKA, V. 2017. Commonly used textile fibers in composite industry for special purposes. *International Journal Knowledge,* 16**,** 1673-1678.

SIMKINS, V., ALDERSON, A., DAVIES, P. & ALDERSON, K. 2005. Single fibre pullout tests on auxetic polymeric fibres. *Journal of materials science,* 40**,** 4355-4364.

SPADONI, A., RUZZENE, M. & SCARPA, F. 2005. Global and local linear buckling behavior of a chiral cellular structure. *physica status solidi (b),* 242**,** 695-709.

STARK, E., BREITIGAM, W., FARRIS, R., DAVIS, D. & STEZENBERGER, H. 1990. Resin transfer moulding (RTM) of high performance resins. *Composite polymers,* 3**,** 423-437.

STEFFENS, F., OLIVEIRA, F. R., MOTA, C. & FANGUEIRO, R. 2017. High-performance composite with negative Poisson's ratio. *Journal of Materials Research,* 32**,** 3477-3484.

STEFFENS, F., RANA, S. & FANGUEIRO, R. 2016. Development of novel auxetic textile structures using high performance fibres. *Materials & Design,* 106**,** 81-89.

SUBRAMANI, P., RANA, S., OLIVEIRA, D. V., FANGUEIRO, R. & XAVIER, J. 2014. Development of novel auxetic structures based on braided composites. *Materials & Design,* 61**,** 286-295.

TALREJA, R. & SINGH, C. V. 2012. *Damage and failure of composite materials*, Cambridge University Press.

TRETIAKOV, K. V. & WOJCIECHOWSKI, K. W. 2007. Poisson's ratio of simple planar 'isotropic'solids in two dimensions. *physica status solidi (b),* 244**,** 1038-1046.

UGBOLUE, S. C., KIM, Y. K., WARNER, S. B., FAN, Q., YANG, C.-L. & KYZYMCHUK, O. 2014. Auxetic fabric structures and related fabrication methods. Google Patents.

UNDERHILL, R. 2014. Defense Applications of Auxetic Materials. *Adv Mater***,** 1-1.

UZUN, M. 2012. Mechanical properties of auxetic and conventional polypropylene random short fibre reinforced composites. *Fibres & Textiles in Eastern Europe*.

UZUN, M. & PATEL, I. 2010. Tribological properties of auxetic and conventional polypropylene weft knitted fabrics. *Archives of Materials Science and Engineering*, 44**,** 120-125.

WANG, X.-T., WANG, B., LI, X.-W. & MA, L. 2017. Mechanical properties of 3D re-entrant auxetic cellular structures. *International Journal of Mechanical Sciences*, 131-132**,** 396-407.

WANG, Z. & HU, H. 2015. A finite element analysis of an auxetic warp-knitted spacer fabric structure. *Textile research journal,* 85**,** 404-415.

WANG, Z., ZULIFQAR, A. & HU, H. 2016. Auxetic composites in aerospace engineering. *Advanced composite materials for aerospace engineering.* Elsevier.

WRIGHT, J. R., BURNS, M. K., JAMES, E., SLOAN, M. R. & EVANS, K. E. 2012. On the design and characterisation of low-stiffness auxetic yarns and fabrics. *Textile Research Journal,* 82**,** 645-654.

YANG, W., LI, Z.-M., SHI, W., XIE, B.-H. & YANG, M.-B. 2004. Review on auxetic materials. *Journal of materials science,* 39**,** 3269-3279.